NTNU – Trondheim
Norwegian University of
Science and Technology

Friction Reduction by using Nano-Fluids in Drilling

Carolin Jahns

Petroleum Engineering
Submission date: February 2014
Supervisor: Sigbjørn Sangesland, IPT

Norwegian University of Science and Technology
Department of Petroleum Engineering and Applied Geophysics

NTNU
Norges teknisk-naturvitenskapelige universitet
Fakultet for ingeniørvitenskap og teknologi
Studieprogram i Geofag og petroleumsteknologi

Study Program in Earth Sciences and Petroleum Engineering
Department of Petroleum Engineering and Applied Geophysics

MASTER OF SCIENCE THESIS

The candidate's name:	Carolin Jahns
Title of Thesis, Norwegian:	Friksjonsreduksjon ved å anvende nano-basert borevæske under boring
Title of Thesis, English	Friction reduction by using nano-fluids in drilling

Extended text:

Recently the oil and gas industry turns to the nanotechnology for innovative solutions to cope with the challenge of ever increasing energy demand. One of the exciting developments in nanotechnology is the discovery of smart nanofluids — a base fluid with suspended nano-sized particles. Nanofluids shed a light on oil well drilling, in terms of modifying rheological properties of fluid, decreasing friction for reduction of drill string torque and drag and mitigating wear on drill string and casing.
Nanoparticles have a typical size range 1-100nm, which induce a large surface to volume ratio. It is reported that nanoparticles offer great lubrication between contact surfaces. The lubrication is mainly attributed to two mechanisms: surface energy change by the adsorption of nanoparticles and ball bearing effect of nanoparticles. However, the friction and wear are strongly temperature dependent due to high interaction between more active atoms at elevated temperature.

Task:

1. Test friction reduction of steel surfaces by using nanoparticle based fluid in different temperature field. Quantify the effect of nanoparticles on friction and wear to reveal the underlying mechanism.
2. Test the friction at different temperature to explore the coupled effect of nanoparticles and temperature.

Different sort of nanoparticles with different size will be utilized and base fluid will be water based fluid.

Supervisor	Sigbjørn Sangesland
Co-supervisor (PPCON)	Jianying He, Dept. Structural Engineering
Studieretning/Area of specialization:	Petroleum Engineering, Drilling Technology
Fagområde/Combination of subject:	Drilling
Tidsrom/Time interval:	September 23 – February 16, 2014

.....
Sigbjørn Sangesland

Abstract

The increasing requirements of drilling fluids in long extended reach wells desires for new solutions to solve torque and drag problems in the wellbore. Nanotechnology is an upcoming technology development, which is already used in other industries to minimize friction coefficients of lubrication fluids in hydraulic hoses. Drilling fluids act also as a lubrication fluid in the wellbore, besides of many other functions it has to fulfill. It is well known that oil based muds (OBM) are characterized with a better lubrication efficiency than water based muds (WBM). Out of this reason, research interest increases about successfully implementing nanoparticles to drilling fluids, especially to WBM, for reducing the generated mechanical friction between drill string and casing.

Within this framework of thesis, tribological and rheological experiments were performed to investigate whether friction reduction can be achieved with alumina, titania or silica nanoparticles. Different particle concentrations in the fluid were tested to see, if lubrication efficiency can be defined to a specific particle concentration. Additionally, the nanoparticle added fluids were tested under different temperature condition to determine the influence on temperature towards nanoparticles.

The experimental phase of the thesis was performed with a pin-on-disk apparatus and a modular compact rheometer (MCR), which allowed tribology and viscosity measurements. The tribology experiments test the metal to metal friction factor, which depend on the lubrication effect of the fluid. The rheology apparatus measures the viscosity of the fluid under different temperatures according to the standardized Fann viscometer. Whereas the pin-on-disk apparatus has an internationalized procedure manual and the test results are assumed to be reliable.

As major result, there is a coupling effect between temperature and nanoparticles in the fluids. With the results of the pin-on-disk apparatus, the titania and silica nanoparticles effectively reduced the friction factor. The alumina particles have a limited friction reduction, in consequence of an increasing friction factor with increasing particle concentration in the fluid.

Preface

This master thesis represents the final part required for the degree of Master of Science (M.Sc.) in Petroleum Engineering in the Department of Petroleum Engineering and Applied Geophysics, at Norwegian University of Science and Technology (NTNU), Norway.

The work of this thesis has been performed in collaboration with the Department of Structural Engineering and the NTNU Nanomechanical Lab.

A base literature research about theoretical relations of friction and drilling fluid components is done in the project "Reduced Mechanical Friction with Nanoparticle Based Drilling Fluids" the semester before. [16] This master thesis is built upon the theoretical explanations and definitions of the project.

The focus of this master thesis is set on experimental testing of tribology behavior during the drilling process. The experiments shall simulate the drill string and casing interaction with nanoparticle added water based fluid as lubricant. Different temperature conditions are tested to find out coupling effects of nanoparticles in drilling fluids and the temperature. In addition, different nanoparticle types are used to analyze their effect on friction and wear behavior.

I hereby declare that I completed this work according to the NTNU regulations, without any improper help from a third party and without using any aids other than those cited. All ideas derived directly or indirectly from other sources are identified as such. This declaration also refers to the representation of figures and visual material.

Acknowledgment

First of all, I would like to thank Roger Overå. He provided support, advice and guidance in the IPT laboratory with the MCR rheometer apparatus. Another acknowledgment goes to Cristian Torres Rodríguez, who helped me in the Nanomechanical Lab.

Special thanks deserves Dipl.-Phys. Andreas Krause, who shared his valuable knowledge of writing scientific reports with me. He guided me especially throughout the end of my project and answered all my questions I had asked. Solving technical bugs, which occured working with LateX, were mainly his merit.

I wish to thank my department supervisor Sigbjørn Sangesland who provided a smooth and straightforward course of my project by organizing and contacting the relevant people for upcoming project tasks. I would also like to thank Jianying He for her support throughout the entire project. Interesting discussions helped me to take decisions regarding the experimental phase of my project.

Finally, I would like to thank Statoil ASA for the opportunity to write this project at their facility in Rotvoll, Trondheim.

Contents

List of Figures

List of Tables

List of Symbols

Δ	Difference.
F_L	Normal Load [N].
F_N	Normal Force [N].
F_R	Friction Force [N].
K	Consistency Index [Pas^n].
L	Length.
M	Torque [Nm].
Φ	Particle Volume Fraction [-].
s	Distance.
V_{loss}	Volume [mm^3].
d_w	Wear Scratch Diameter.
η	Viscosity [Pas].
f	Friction Coefficient [-].
$\dot{\gamma}$	Shear Rate [s^{-1}].
γ	Shear Strain [-].
μ	Friction Factor [-].
n	Flow Behavior Index [-].
ϕ	Deflection Angle [°].
rpm	Rotation per Minute.
r_{sp}	Radius of the Spherical Shaped Pin.
r_w	Wear Scratch Radius.
r	Radius.
σ	Stress Distribution.
τ	Shear Stress [Pa].
v	velocity [m/s].

List of Acronyms

BB barite, bentonite.

BBP barite, bentonite and polymer.

ECD equivalent circulation density.

HEC hydroxyethylcellulose.

HPHT high pressure high temperature.

IPT Institut of Petroleum Technology.

MCR Modular Compact Rheometer.

NTNU Norwegian University of Science and Technology.

OBM oil based mud.

STLE Society of Tribologists and Lubrication Engineers.

TEM transmission electron microscopy.

WBM water based mud.

List of Subscripts

avg	Average
b	Bob
c	Cup
yp	Yield Point
pl	Plastic
eff	Effective
s	Sliding
sp	Spherical
w	Wear

Chapter 1
Introduction

Nowadays, nanotechnology is introduced into the oil and gas industry to further increase the efficiency of established processes. Applying nanoparticles for reservoir stimulation is only used in exceptional cases, because the technology is very pricy. Another possible field of application in the oil and gas industry could be in the drilling process. Nanoparticles as components in drilling fluids could potentially reduce mechanical friction, which is generated between the drill string and the casing. The interest of using the "smart drilling fluids" increases steadily. Many benefits can be derived from colloidal suspended fluids. One advantage is that the total amount of larger particle components can be reduced. A higher surface area of smaller particles requires a reduced concentration, because the surface volume of nanoparticles is high. The same functions a drilling fluid provides can be achieved with a smaller particle concentration. A lower total particle concentration reduces the hold down effect of the drilling fluid. [7]

This master thesis is based on the literature research done in the semester project: "Reduced Mechanical Friction with Nanoparticle Based Drilling Fluids". Former research and the state of the art development has been introduced in that project. There, it was pointed out that there is a high potential in using nanoparticles in oil based mud (OBM). Nanoparticles are supposed to contribute to the reduction of friction by acting as ball bearing between the metal surfaces or create a smear film between the surfaces due to reaching of the material specific melting point. [19] On this theoretical evaluation, the experimental series are based and selected to evaluate the practical implementation.

Nanoparticles in drilling fluids could possibly act as lubrication additive. In this project, the possible friction reducing process will be experimentally investigated and evaluated. A commonly used drilling fluid for reducing friction is OBM, because it provides good lubrication compared to water based mud (WBM). [22] This is due to the nonpolar characteristical property of oil, which allows that particle movements occur without any particle attraction or repulsion. WBM is an ionic fluid and is

naturally charged, which influences the lubrication properity. Out of this reason water is by nature a less suitable lubricant. On the other hand, water is environmental friendlier. On the Norwegian continental shelf, the first top hole section are required to drill with WBM and is commonly used as long as borehole conditions allows. Therefore it is of particular interest to investigate and improve lubrication behavior of WBM, with the help of nanoparticles. [1] Additionally, the influence of temperature of fluids with nanoparticles shall be investigated to specify the fluid behavior under higher temperatures.

The MCR apparatus is an available testing equipment, which allows tribology and rheology measurements. For each measurement purpose a different measurment cell can be installed to the apparatus. In addition, for a limited number of tests is available the international standardized pin-on-disk apparatus.

This thesis explains the experimental setup for both tribology measurement tools. The MCR apparatus will be used prior to the pin-on-disk apparatus to observe possible temperature influences on nanoparticle behavior in the fluid and to define benefitial particle concentrations. Based on these results the pin-on-disk test series has been performed. This allows a conclusion whether the MCR apparatus is a suitable measurement equipment and the investigation can be backed by the pin-on-disk results.

The focus of the research is to find a good particle concentration in the fluid to optimize the lubrication and to compare different material types to compare their tribology behavior. In addition, the influence of a possible interaction between polymers and nanoparticles can be investigated, as well as the relation between temperature and nanoparticle added fluids.

First, the fundamental tribology and rheology chapter shall complement the literature reseach from the semester project. The following chapter introduces the required mathematical foundation of the used pin-on-disk apparatus and the MCR instrument. Subsequent, the detailed methodology of the testing instruments and the handling procedures are explained. The main results are exemplified afterwards.

Chapter 2
Fundamentals of Tribology and Rheology of Drilling Fluids

Tribology is the science which describes the friction behavior between elements. Friction occurs when elements are in close contact and their particles or surfaces interact with each other and create a drag force. In dependence of the material abrasiveness, asperity and shape, friction can be decreased or increased. [11] Since any interaction of materials will cause friction and different material hardness results in or has an influence of each other's surface structure, tribology is directly linked to wear. The choice of the material, the amount of friction and type of the material movement, the material surface interacts differently. With increasing friction the material wear increases proportionally. Wear is defined as the loss of material due to any form of created friction. Friction between to material surfaces is named external friction or mechanical friction. Internal friction occurs between the particles of the material itself. The mechanical friction behavior between two materials is adressed in this report.

Rheology describes the behavior of fluids. The typical drilling fluid used in the oil and gas industry shows a shear thinning behavior with applied shear stress. This phenomenon is called thixotropy. It is also important to analyze the rheological behavior when nanoparticles are added to the base fluid, since the general functions of drilling fluids have to be maintained and ensured. It is relatively new in the industry to intentionally add colloidals to the drilling fluid. Therefore it is of high importance to know the influence on viscosity and the particle impact in rheology as it changes with different temperature environments.

2.1 Wear mechanisms

Wear mechanisms are roughly divided into adhesive and abrasive wear mechanisms. Other types of wear are corrosion and fatigue. [18] Abrasive wear defines the frictional movement between two or more elements where at least one element is physically harder than the others, this creates a volume and mass loss at the softer of these rubbing elements.

Abrasive wear is of particular interest for this case study, because it includes the sliding and impact movement, which are both present during drilling. The mechanism of abrasive wear is illustrated in figure 2.1 on the left picture. Derived forms of abrasive wear are machining, grinding and polishing. During the testing phase with the pin-on-disk apparatus, abrasive friction will be the major wear mechanism of concern. Adhesion wear is more linked to cold welding, due to high pressure impact between two surface elements. One special form is called galling. To illustrate both wear mechanisms, figure 2.1 shows the abrasive wear mechanism on the left picture and the galling process on the right picture. [17] [18]

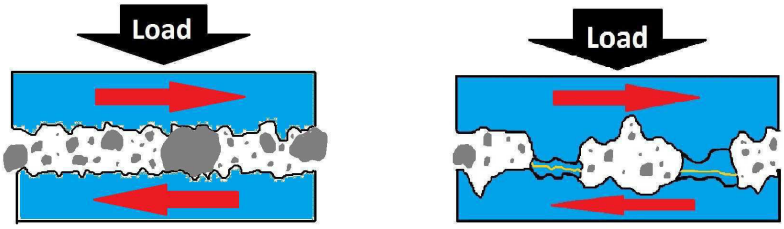

Figure 2.1: Left picture: Abrasive wear mechanism; Right picture: Illustration of galling, an adhesive wear mechanism

Another type of wear is fatigue wear. It describes the repeated impact of friction to the surface element until a surface crack spreads out and reaches deeper parts of the material, which can lead to a complete material failure. Fatigue wear typically occurs after long term usage. Corrosion as a chemical wear mechanism is of interest, because WBM will be used as the base fluid for analyzing the effect of nanoparticles as lubricant. Corrosion is a wear mechanism which occurs in water, oil and under air conditions. It is a time dependent chemical reaction. Water provokes corrosion at untreated steel surfaces due to its high amount of ions. Steel corrosion in contact with water will always occur and varies by the amount of ions in the water. [2] Commonly used steel grades for drill pipes are not stainless steels and are therefore affected by corrosion. Corrosion adversely affects the material surface and changes its properties and asperity.

According to Ingrid Kjellevoll [17] polishing wear has the most least impact of all wear mechanisms. Wear during the drilling process occurs to the drill string and its single components like stabilizers, tool joints, cross over subs and casing. The aim to reduce the degree of wear and to increase the lifetime of these components, the drilling fluid has to improve its function as lubrication fluid. With decreasing gap between drill string and casing, the influence of the drilling fluid as mechanical friction reducer decreases. According to the Stribeck curve [16], lubrication stages change with the decreasing distance between surface elements, from hydrodynamic lubrication to boundary and thin film lubrication. The smaller the gap is, the more mechanical friction occurs and wear to the steel pipe and hydraulic lubrication can be neglected. A well suited drilling fluid as lubricant should be able to minimize all four wear mechanisms: abrasive, adhersive, fatigue and corrosion wear.

2.2 Parameters Influencing Tribological Behavior

The composition of the fluid assigns the tribological behavior and significantly specifies its ability as lubricant. The influencing parameters from the previous semester project is summarized as follows. The tribological behavior depends on:

- the size of the particles,
- the shape of the particles,
- the concentration of the particles,
- the particle solidness,
- the forces acting on the materials,
- the material properties like abrasiveness (asperity),
- the time frame of the material contact and
- the base fluid e.g. water or oil.

The larger the particle sizes in the drilling fluid/lubrication fluid are, the larger is the impact of abrasive wear towards the material surfaces. Figure 2.1 illustrates that big particles act as a third element component during the movement process and have a larger destructive surface influence. Not only the size, but also the shape of the particles influences the degree of surface wear. Sharp edged particles interact more with material asperity than rounded edges or spherical shaped particles.

The concentration of the fluid additives defines the interaction between all other particles in the fluid and the higher the concentration is, the higher is the contact time towards the material surfaces. The interaction strongly depends on the fluid film thickness between the elements. Additionally to the fluid components, the cutting transportation can not be neglected. Here the particle sizes are constrictivly changeable and the concentration of cuttings at certain sections of the well depends largely on the dogleg severity of the oil well.

Different forces like torsional force, lateral force and hydraulic pressure act on the casing from the drill string and the drilling fluid. The mechanical forces require a certain solidness of the particles. Particles like the planned nanoparticles in the drilling fluid are supposed to act as ball bearings between two elements like the drill string and the casing. When high forces overcome the specific solidness of these particles, the effect vanishes.

Nevertheless, the biggest impact on the efficiency of a lubricant is the base fluid as shown in table 2.1. OBMs are known to be good lubricants, whereas water based fluids perform less efficient as lubricants. [22] Regardless to this fact, water based fluids are the most common used fluids while drilling in top hole sections and have to be compulsory used in the first top hole sections in the Norwegian continental shelf.

Table 2.1: Friction factors in cased holes and open holes depending on the drilling fluid [22]

Drilling Fluid Type	**Friction Factors**	
	Cased Hole	Open Hole
Oil based	0.16 - 0.20	0.17 - 0.25
Water based	0.25 - 0.35	0.25 - 0.40
Brine	0.30 - 0.40	0.30 - 0.40
Polymer based	0.15 - 0.22	0.20 - 0.30
Synthetic based	0.12 - 0.18	0.15 - 0.25
Foam	0.30 - 0.40	0.35 - 0.55
Air	0.35 - 0.55	0.40 - 0.60

2.3 Rheology

Rheology is the study of the flow and deformation of fluids. It is of interest, because the knowing fluid properties like viscosity and yield points defines the field of applications of a drilling fluid. Thixotropic fluids, like drilling fluids, are characterized by a specific initial yield stress. [20] Non-Newtonian fluids have a non-linear relationship between shear stress and shear rate and are commonly mixtures of liquid phases (here: the base fluid e.g. water or oil) and with a solid phase (here: the fluid components e.g. barite and bentonite). A non-linear fluid behavior means that the fluid component particles behave differently to each other when the amount of shear rate changes. [23] A high quality drilling fluid is defined by building up a good gelling structure at decreasing pumping rates, which implies a low shear rate. On the other hand, with an increasing pumping rate the gelling structure will be destroyed and the shear stress decreases. That phenomenon supports the cutting transportation out of the borehole and keeps them in suspension during circulation stops.

Every component in the drilling fluid has its impact on the total fluid behavior. Adding nanoparticles to the drilling fluid will also affect the characteristical rheology behavior. It is important to analyze an appropriate volume fraction Φ for nanoparticles, because the aim is to figure out an optimal concentration for reducing friction in the borehole. Additionally, it is important to minimize the effect on viscosity. A high viscosity implies a higher required shear stress before the fluid starts moving again after a circulation stop. This issue reflects the limitation of today's pumping systems and long distance boreholes, which are characterized by narrow pressure windows.

Viscosity η is the ratio of shear stress τ to the shear rate $\dot{\gamma}$, see equation 2.1 [24]. Generally, viscosity depends strongly on temperature, because with increasing temperature the particle movement increases and by that their interaction with each other. The viscosity of drilling fluids usually decreases with increasing temperatures and the electrochemical as well as the chemical reactiveness of the fluid with clay particles might increase. [23] Therefore it is expected that adding nanoparticles will have an impact on fluid viscosity and the initial yield stress, especially due to the flocculation and agglomeration tendency of the drilling fluid components like clay. Due to this reason a long intermission of the pumping should be avoided. High quality drilling fluids are also well dispersed fluids without segregation of its solid components.

Newtonian model:

$$\eta = \frac{\tau}{\dot{\gamma}} \tag{2.1}$$

In general, there are two major types of fluids: Newtonian fluids and Non-Newtonian fluids. Newtonian fluids are defined by a linear relation between shear stress τ and shear rate $\dot{\gamma}$, whereas Non-Newtonian fluids exhibit a non-linear relationship. Several fluid models apply to drilling fluids: the Bingham model, the Power law model and the Herschel Bulkley model to name the most familiar ones. Simple fluid composition rheology can be expressed with either the Bingham or the Power law model. Both models are defined by the equations 2.2 and 2.4. Both models require two data points at high shear rates and are relatively imprecise at low shear rates. Nowadays increasing borehole length challenges also the drilling fluid properties due to tight pressure windows or high pressure high temperature (HPHT) conditions. Out of this reason the complexity of the fluid composition rises rapidly. More complex rheology investigations are better represented with for instance the Herschel Bulkley model, represented in the equations 2.7. It requires three data points, because of three unknown variables in the formula. [24]. The symbols in the equations represent the following parameters: τ is the shear stress, τ_{yp} is the yield point stress, η_{pl} is the plastic viscosity, $\dot{\gamma}$ is the shear rate, K is the consistency index and n is the flow behavior index.

Bingham plastic model:

$$\tau = \tau_{yp} + \eta_{pl}\dot{\gamma} \tag{2.2}$$

The plastic viscosity η_{pl} can be calculated with the equation 2.3:

$$\eta_{pl} = \frac{\tau_{600} - \tau_{300}}{\dot{\gamma}_{600} - \dot{\gamma}_{300}} \tag{2.3}$$

Power law model:

$$\tau = K\dot{\gamma}^n \tag{2.4}$$

n can be calculated from:

$$n = \frac{log\ \tau_{600} - log\ \tau_{300}}{\dot{\gamma}_{600} - \dot{\gamma}_{300}} \tag{2.5}$$

K can be calculated from:

$$K = \frac{\tau}{\dot{\gamma}^n} \tag{2.6}$$

Herschel and Bulkley model:

$$\tau = \tau_{yp} + K\dot{\gamma}^n \tag{2.7}$$

The yield point τ_{yp} can be solved graphically or assumed to be $\tau = 3\ Pa$. After knowing n from the graph slope, K is simply calculated.

K can be extracted from:

$$K = \frac{\tau_2 - \tau_1}{\dot{\gamma}_2^n - \dot{\gamma}_{yp}^n} \tag{2.8}$$

The graph in figure 2.2 [24] illustrates the typical different flow curves of the above mentioned models. While mixing a drilling fluid and testing it, a flow curve can be plotted and the correct fluid model can be applied to describe the fluid properties

at certain conditions. This can provide the necessary fluid behavior under certain conditions and allows the fit for purpose application of drilling fluids while drilling.

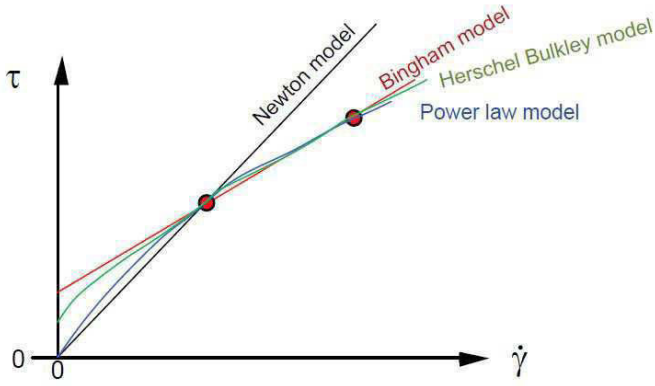

Figure 2.2: Rheology models

2.3.1 Brownian Motion Theory

The analysis of colloidal suspended fluids includes the Brownian motion theory. The theory describes the interaction and motion of suspended particles in a fluid. According to Jan Mewis and Norman J. Wagner et. al. [20], a low volume fraction $\Phi < 0{,}5$ in a fluid with one type of particle, all particle interactions can be neglected. But drilling fluids usually have a much higher fraction than 0.5 and contain more than one component. The Taylor expansion in equation 2.9 allows to describe the effective viscosity η_{eff} of a fluid more precisely. C_2 as the coefficient in equation 2.9 reflects the impact force of other particles in suspension and the hydrodynamic influence of the fluid. It shall also be mentioned that spherical particles rotate with the fluid flow. [20] This is particularly interesting, since the planned nanoparticles for the laboratory test have a spherical shape and shall theoretically act as ball bearings between the two material elements.

$$\eta_{eff} = 1 + 2,5\phi + c_2\phi^2 + c_3\phi^3 + ... \tag{2.9}$$

Anyway, particle flocculation and segregations should be prevented, because flocculated fluids change again the fluid rheology. A change in pH value can be a countermeasure for interparticle attraction. It is commonly imperative the higher the pH value is the lower the colloidal flocculation tendency of the particles. Another aspect is the electrostatic attraction, which depends on the surface charge of the particles. Especially polymers can influence the degree of flocculation, since high

molecular weighted polymers induce the process of flocculation due to their length and surface charge, called the steric force.

Colloidal particles are characterized by their high surface to volume ratio and are therefore especially sensitive towards surface attraction. If a certain fluid particle concentration is reached, the particle interaction rises and van-der-Waals forces dominate the particle attraction behavior. Aggregation occurs, which has to be avoided. Particle aggregation is usually an irreversible chemical reaction. Figure 2.3 pictures the impact of salt on electrostatic attraction within a fluid system. Salt is a highly ionic component, which impacts the surface charge and reactiveness of other fluid components. A possible countermeasure could be a short anionic polymer for neutralizing the electrostatic imbalance. [24]

Summing up, colloidal particles are very prone to flocculation and aggregation due to their size. Preventing this, an equilibrium of electrostatic, steric and electrosteric forces can minimize this effect. [20]

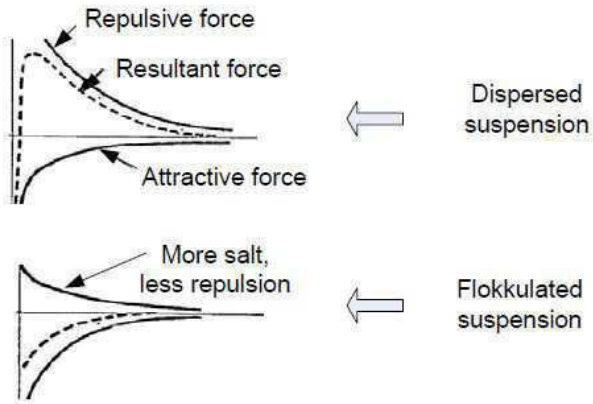

Figure 2.3: Electrostatic forces and van-der-Waals forces on suspended fluid particles [24]

2.3.2 The Effect of Temperature to Fluid Rheology

The book of Ryen Caenn (2011) [23] describes well the temperature effect on the fluid rheology. In this context, figure 2.4 presents the possible temperatures a drilling fluid can go through. The surface temperature (80°F = 26°C) is the stage where the fluid will be mixed together and pumped down the borehole up to a depth of 20000 ft. = 6097 m to reservoir temperature and pressure (350°F = 176°C). After that the fluid is pumped back to the surface through the annulus. During the circulation the fluid is additionally exposed to circulation stops, which can last from a couple of minutes to hours. Drilling fluids are thixotropic fluids, because of the clay content in the fluid. Thixotropic fluids in motion are characterized by their liquid phase and by their gel structure building phase during the time of rest. This effect is associated with the clay particles in suspension in the state of motion. During circulation stop the clay particles start to flocculate due to their surface charge (electrostatic attraction) and build up the gel structure. This is the stage when viscosity of the drilling fluid increases with the aim to keep cuttings and other particles in place. When the gel strength is fully developed the applied shear stress has to be overcome first before the fluid breaks its gel structure and starts to flow again. In this case, it is the yield point shear stress τ_{yp} of the fluid. Thixotropy is time and shear rate dependent. The fluid capability to build up such a gel structure changes with temperature. With it changes also the viscosity of the fluid at different fluid stages. Temperature impacts the properties of the fluid as following: [23] [14]

1. A temperature elevation leads to a lower viscosity of the drilling fluid. Contrary to this, a usually interconnected increase in pressure causes a fluid compression, which results in a viscosity gain. Commonly the temperature effect dominates the pressure impact for water based fluids. [14]

2. Increasing temperatures entail a higher activity lever of metal hydroxides (negatively charged) with the clay particles in the drilling fluid. It accelerates the gel structure formation even though the fluid phase is in circulation. H.C.H. Darley (1956) [14] found out that barium hydroxide would be an optimal substitution to the conventional calcium hydroxide additive to reduce the effect to a possible minimum.

3. Additionally to the increase of the hydroxide activity, the activity of electrolyte rises. As mentioned in the previous section, electrochemical attraction and repulsion between particles and their surface charge is elevated and causes a faster aggregation development in the fluid. [14]

However, the temperature influence towards the fluid depends on three major aspects of the well: the pumping rate, the fluid type and the wellbore depth and

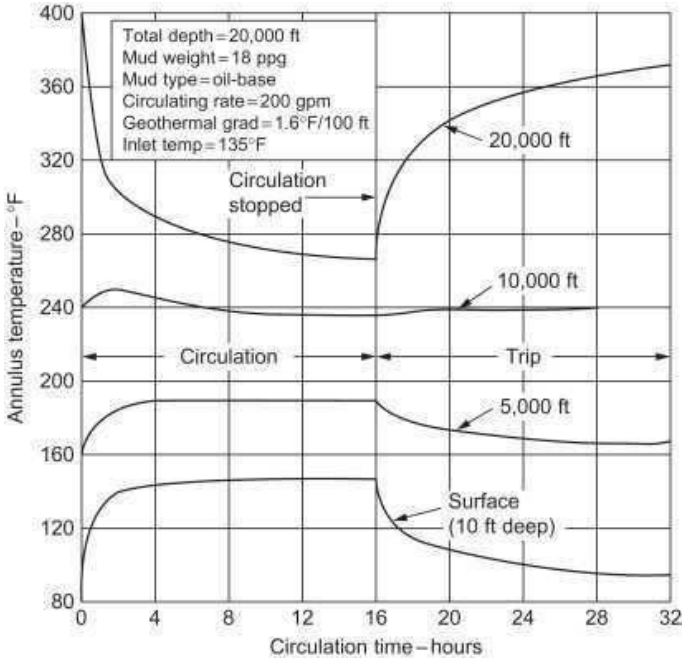

Figure 2.4: The effect of temperature to the fluid rheology in a borehole. [23] Courtesy of Raymond (1969) [21]; Copyright 1969 by SPE-AIME

all three factors are limited modifiable. [21] The pumping rate is known to be a critical aspect and can be interrupted during tripping or work over tasks. A good balance of high pressure pumping and low pressure pumping is important, not only due to the developing temperature equilibrium during slow circulations. Cutting transportation has to be ensured and is mainly influenced by the pumping rate. It cleans the borehole and therefore results in a faster drilling penetration. On the other hand, a large circulation rate increases the equivalent circulation density (ECD) at the bottom of the well and might lead to pressure window problems.

According to H.C.H. Darley (1956) [14] the temperature conditions in a wellbore have greater impact to WBM compared to OBM and the pressure influence is minimal. Temperature equilibrium is by trend rather achieved in WBM than in OBM. The conclusion is that the fluid composition of WBM should be more resistant to higher temperatures than OBM. But practically it is less resistant due to the electrochemical and chemical responsiveness. The exposed fluid temperature depends on the borehole length. The longer a wellbore, the larger the temperature impact is, due to the temperature gradient. Usually WBM is used at the first borehole sections and is replaced with OBM in higher depth and higher temperature environments. For OBM applies the opposite, the temperature effect is relatively low, but the pressure impact

is higher. But OBM shall not be further discussed here.

The fluid phase for the moment has a great impact on the stability of a drilling fluid in high temperature situations. Hiller et.al. (1963) found out that when a well suspended WBM is exposed to high temperatures the plastic viscosity decreases. But as soon as agglomeration of the clay containing fluid begins both curves behave different from each other. The plastic viscosity behaves as expected and decreases with higher applied shear rate, but the yield point curve increases exponentially as soon as the temperature rises above 100°C. [8] [15] [23] The yield point is a fluid specific value, which depends on the composition of each fluid. Therefore a prediction and general expression for water base drilling fluid behavior is difficult to establish.

Chapter 3
Tribology and Rheology Measurement Setup

Several instruments are available to perform tribology measurements in the laboratory. To allow the comparison of tribology results, some experiment setups are qualified for international standards. The testing procedure has to be individually adjusted to the specific laboratory conditions and existing instruments. It is difficult to set standards, because tribology measurements imply several lubrication stages like the thin film lubrication, boundary lubrication, mixed lubrication and hydrodynamic lubrication stage. These lubrications stages are not visible with the eye and parameters impacting the tests in the laboratory are different to the reality and might be only either removable or observable in the laboratory. Thin film and boundary lubrication are in particular sensitive towards external factors like minor vibrations of the building, air humidity changes or environmental sounds. [13] For comparable results and meaningful measurement reasons, it is important to be aware of the importance of consistent sample preparation for each test procedure. [13]

During the experimental phase of this thesis, international standardized procedures are used for the pin-on-disk apparatus with the ASTM G99-05 (2010) standard. This standard procedure manual describes in detail step by step the experimentsal procedure. It defines the orientation, the alignment of the testing equipment, the execution of the tests and how the results should be reported. [12]

Another but not standardized test is the MCR modified tribology measuring cell of an Anton Paar apparatus. This instrument allows a static friction test, where a concentric rotating steel ball moves along three steel plates, which are fixed to a sample plate holder filled with the testing fluid. [10] Temperature, sliding speed and normal force as well as other parameters and testing conditions can be chosen and varied depending on the observation goal. Both tribology measurement results can be theoretically compared by the amount of changing friction factors.

Measuring the rheology of a fluid is commonly done with a viscometer. The MCR is equipped with a suitable modification apparatus for a viscometer measurements

cell, which is able to measure fluid viscosities. A viscometer is designed with a rotating cylinder in a fluid filled cup, which creates a shear flow in the cup. The resulting forces and momentums acting on the cylinder, also called bob, provide the data to measure the fluid specific shear rate and shear stresses at a specific rotational speed. Plotting both parameters in a diagram will provide a fluid specific flow curve, which defines the plastic viscosity. [23]

3.1 General Wear Equations

There exist many wear models and equations to express the process of lubrication. In this chapter only the equations are introduced, which are directly linked to the laboratory testing series. The pin-on-disk apparatus and the ball-on-three-plates principle of the MCR equipment will be used for the tribology experiences. Both instruments test the friction factors and with it the lubrication efficiency of the sample fluid.

3.1.1 Pin-on-Disk Apparatus

The pin-on-disk apparatus is an often used measurement tool to investigate and observe the lubrication behavior. The standardization manual ASTM G99 and DIN 50324 defines the exact procedure. The apparatus is equipped with a one sided open cylinder (called disk) where the material sample can be installed with a sample holder frame. A schematical drawing of the function of the pin-on-disk is shown in figure 3.1. Several types of pin-on-disk apparatus exist, but the basic function is the same. A cylindrical shaped pin or a spherical shaped pin is pushed with a changeable force onto the material sample. The rotational diameter can be determined prior to the start of the test. According to the rotational diameter, the sliding distance and sliding speed can be adjusted. More advanced instruments also allow a temperature modification for the testing series. All type of lubrication liquids can be used for this apparatus.

Starting with the pin-on-disk measurements, the wear is measured by the calculated volume loss of either the pin or the disk. It is assumed that only one of these parts is significantly damaged whereas the damage to the other part is insignificantly affected. If the disk or pin is the part with the lower material strength, the particular element will be analyzed in more detail. A suitable confocal microscope allows measuring the exact diameters d_w or radiuses r_w of the scratches created on material surfaces. The radius r_{sp} of the spherical shaped pin also has to be measured to include the impacting contact area. The calculated volume loss V_{loss} represents the degree of wear on the material. These formulas are according to the ASTM standard. [12] The pin volume loss is calculated with the equation 3.1. Here it is assumed that the disk volume loss is negligible.

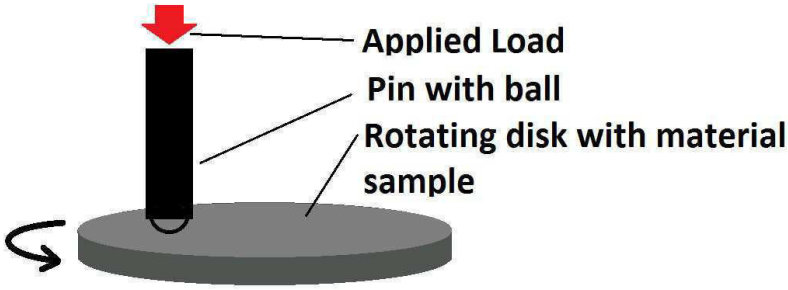

Figure 3.1: Schematical drawing of the pin-on-disk measurement principle. The pin is pushed on to the rotation disk with the lubricant. By that, scratches occur on the surface, which are used to extract the relevant paramters.

In case that the pin has a neglectable abrasion, equation 3.3 is valid for the analysis of the disk volume loss.

Wear Groove Volume

As indicated above, with the help of a confocal 3D microscope, the wear grooves can be visualized and measured. This is an indication of the amount of material loss and the friction.

$$V_{loss\,pin} = \frac{\pi h}{6}\frac{3\,d_w^2}{4+h^2}\ \ [mm^3] \tag{3.1}$$

where h is calculated accroding to equation 3.2:

$$h = r_{sp} - \left(r_{sp}^2 - \frac{d_w^2}{4}\right)^{\frac{1}{2}} \tag{3.2}$$

The volume loss is calculated according to equation 3.3:

$$V_{loss\,disk} = 2\pi r_w\left(r_{pin}^2 sin^{-1}(\frac{d_w}{2r_{pin}} - (\frac{d_w}{4})(4r_{pin}^2 - d_w^2)^{\frac{1}{2}}\right)\ \ [mm^3] \tag{3.3}$$

3.1.2 MCR - Tribometer Measurement Cell

The tribology tests with the MCR - Tribometer Measurement Cell allow the measurement of the friction and lubrication properties of fluids. Adjustable parameters are the normal force, rotational speed, temperature, distance of the zenith of the steel ball and the bottom of the testing apparatus. The sliding speed corresponds to the rotational speed of the measuring system. Possible standard measurement applications in the software are either the Stribeck curve or a static friction test, where the torque is steadily increasing. The fundamental setup for the experiments is performed at room temperature and atmoshpheric pressure. The MCR automatically recognizes which type of measurement cell application is installed to the apparatus. [10]

The tribology measuring principle bases on the ball-on-three-plates principle, shown in figure 3.2. The schematic illustration of figure 3.2 shows the ball fixed into the shaft, which pushes down towards the steel plates with a specific normal force. The contact points of the ball and the plates depend on the deflection angle α of the steel plates and define also the distance d between the zenith of the steel ball and the contact point. As soon as the steel ball and shaft are lowered, the experiment starts and the shaft rotates around its own axis. The gap between the steel ball and the bottom of the sample holder can also be adjusted and ranges commonly from $0\ mm - 5\ mm$, but can be set larger. For each test three new steel plates and a new steel ball are installed to the apparatus. In figure 3.3 it shows that the three sample plates are screwed to the sample holder. The sample holder is also screwed onto the MCR apparatus, so that unwanted movements are prevented, which could interrupt and destroy the measurements. The sample ball is pressed into a shaft, which prevents any rotation of the ball itself.

For any friction test it is of particular importance that the testing material is clean and has not been in contact with other than the testing fluid. Wearing gloves is one requirement to protect the equipment from contamination.

The tribology test with the MCR instrument calculates the friction coefficient based on the following formulas. With a defined normal force F_N of the rotating steel ball and the measured deflection angle α, the sample specific normal load F_L can be determined, in equation 3.4. Together with the calculated friction force F_R, which depends on the momentum M, the radius r of the steel ball and the deflection angle α (equation 3.5), the needed friction factor μ can be estimated (equation 3.6). The MCR apparatus is able to apply a normal load of maximum 50 N, which is equal to a friction force of 70 N [10].

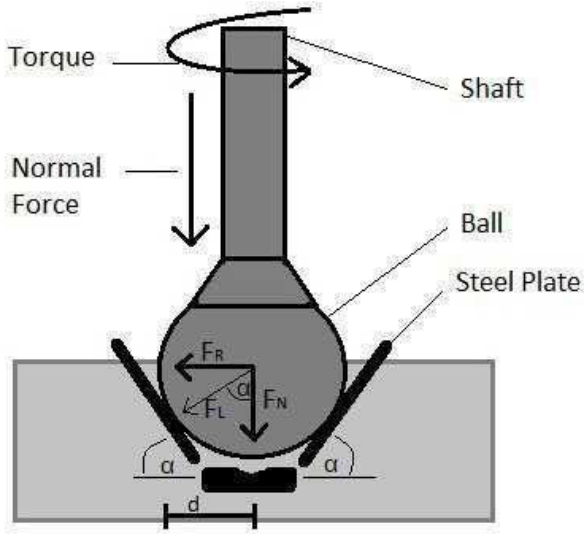

Figure 3.2: Friction measurement schematic of the MCR 302 SmartPave apparatus.

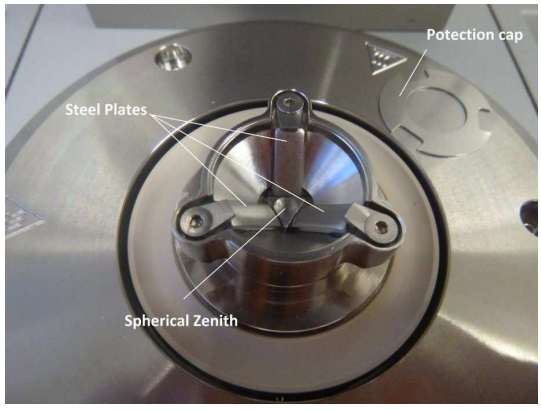

Figure 3.3: Three steel plates in the friction apparatus of the MCR.

Normal Load

The perpendicular force between the ball and the three sample plates is called normal force. The normal force is variable for all experiments and can be prior set as a constant or steady increased or decreased value during the experimental series.

$$F_L = \frac{F_N}{cos\alpha} \tag{3.4}$$

Friction Force

The friction force is calculated based on the changing momentum. Radius r and the deflection angle α are constant for each experiment, because the size of the steel ball remaines the same for all experiments. The distance of the steel ball zenith and the bottom of the basin is constant. The material sample holder requires the same shape and thickness for each steel plate.

$$F_R = \frac{M}{r \cdot sin\alpha} \tag{3.5}$$

Friction Factor

The friction factor is equal to the friction force divided by the friction load and is therefore a dimensionless number used in fluid mechanics. It expresses the quality and efficiency of a lubricant. The lower the friction factor is, the better the lubrication and vice versa for high friction factors.

$$\mu = \frac{F_R}{F_L} \tag{3.6}$$

Sliding Speed and Sliding Distance

For illustrating a Stribeck curve it is required to know either the exact sliding speed v_s or sliding distance s_s. The graph will illustrate the friction behavior changes over a period of time and the effect of distance. Equation 3.7 and 3.8 clarify how the deflection angle φ, the radius r of the steel ball and the rotation of the steel ball n impact these two parameters. The sliding speed depends on the rotation of the steel ball and with it on the momentum. Because the momentum slightly fluctuates, the sliding speed varies too.

$$v_s = \frac{2\pi}{60} \cdot n \cdot r \cdot sin\alpha \tag{3.7}$$

The sliding distance expresses the contact duration of two materials. This length usually results in a sample specific mass loss, which can be analyzed by the wear groove which is formed.

$$s_s = \varphi \cdot r \cdot sin\alpha \tag{3.8}$$

The measurement cell has an integrated heating chamber, which allows to vary the sample temperature from - 40°C to 200°C. It enables a room temperature independent experimental environment. The heating and cooling feature requires a cooling system prevents the apparatus from over temperature. [10]

3.2 Rheology Measurements

A viscometer measures the fluid behavior under applied shear forces. More specific, it determines the rheology characteristics according to the drag force of the fluid. The viscometer is equipped with a bob and a cylindrical cup, shown in figure 3.4. The cup is filled with the sample mud and the bob enters the basin completely and starts rotating. The rotation acts on the drilling fluid with a shear force and creates a drag force. The drag force varies in dependence on the fluid state prior to the rotation. If the fluid has been in motion, the drag force will decrease. If the fluid rests for a while, the drag force will be significantly higher for thixotropic fluids. In the section 2.3, more details about the factors, that influence the fluid rheology, are described in detail.

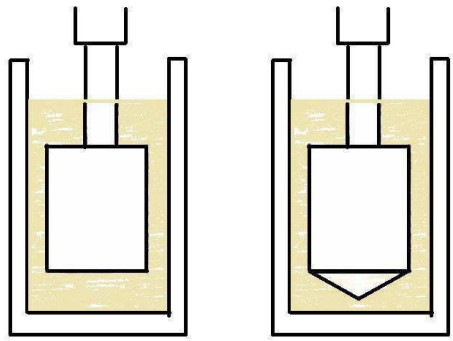

Figure 3.4: Schematical drawing of a viscometer with cylindrical bob used for OBM (left picture) and a bob with cone used for WBM (right picture).

Permanent changes of the fluid properties require a continuous observation of the fluid properties on the rig side to ensure constant drilling fluid quality with the

formation. The changes are from chemical reactions and temperature fluctuations. The Fann viscometer can be found on every rig side in the world. It supports six standard rotational speeds: $3, 6, 100, 200, 300$ and 600 rpm. The high range of rotation speeds is attributed to the high range of shear stress in practice. Low shear stresses occur during the startup of the fluid circulation and at the pipe and borehole wall. Medium high shear stresses appear in the center between the two surface walls and at narrow flow diameter situations. The high shear stress (up to 600 rpm) reflects the shear force acting on the fluid in the nozzle section of the drill bit, where the drilling fluid has to pass. [23] More advanced viscometers allow a temperature regulation of the fluid sample and the testing equipment.

The measured data is plotted in a flow curve, as shown in figure 2.2. Changes in fluid rheology during drilling can be observed by comparing these curves. Those changes can be counteracted, when e.g. a high reactive formation is drilled. The MCR apparatus is another type of viscometer, shown in figure 3.5.

A viscometer is another term for the concentric cylinder system. The fluid dynamics in a borehole are somewhat similar to the viscometer instrument dimensions. The bob and the cylindrical basin form an annulus between each other and the bob rotation simulates the drill string rotation in a vertical borehole. Understanding the stress distribution of the instrumental set up allows to analyze the influence of torque M, length of the bob L and radius of the gap r to the results. [20]

$$\sigma(r) = \frac{M}{2\phi L r^2} \tag{3.9}$$

When the condition in equation 3.10 is fulfilled, the average shear rate value can be calculated with the equation 3.11.

$$\frac{r_b}{r_c} > 0,99 \tag{3.10}$$

$$\dot{\gamma}_{avg} = \frac{M \cdot r_{avg}}{r_c - r_b} \tag{3.11}$$

and the average radius is:

$$r_{avg} = \frac{r_c + r_b}{2} \tag{3.12}$$

The advantages of the viscometer measurements are that no leakage occurs at high shear rates. Additionally during temperature regulated measurements, the

Figure 3.5: Modular Compact Rheometer (MCR) with mounted viscometer measurement equipment. The viscometer is visible as the bob and cup part of the MCR apparatus.

temperature distribution is uniform in the entire cylindrical basin. The dehydration of the fluid sample is minimal. The disadvantages of such a test are the possible containment of air bubbles into the samples. [9]

Chapter 4
Methods of Experimental Testing

The main tribological measurement instruments are provided by the TibologyLab of Norwegian University of Science and Technology (NTNU) and SINTEF in Trondheim. The available apparatus for this project is a pin-on-disk apparatus, which enables experiments according to the ASTM International Standard G99 and DIN 50324. The MCR 302 SmartPave manufactured by Anton Paar has several modification possibilities that helps to analyze rheological and tribological properties of nanoparticles in drilling fluids. One feature is that conventional viscosity measurements can be performed. An additional modification set named *Tribology System (T-PTD 200)* enables tribological tests based on a ball-on-three-plates principle. [10]

With regard to the fluid composition and nanoparticles as a possible additive. Nanoparticles belong to the category of colloidals. Colloidal suspensions are characterized by their particle interaction and affect fluid viscosity. Colloidal suspensions are supposed to behave different compared to conventional fluid compositions. The aim of this work is to observe how nanoparticles modify the rheological properties of the drilling fluid. For that, different temperatures are applied to the colloidal suspension during measurement. This initiates the conditions of the fluid under drilling conditions. By being able to reduce friction with nanoparticles in drilling fluids, it could be also possible to reduce material wear of the drill pipe. Analyzing the amount of lost material gives a conclusion about the friction interference between two materials.

4.1 Fluid Composition

The base fluid is mixed manually in the laboratory out of the seperate components. The testing fluid will be a WBM, which is commonly used in the industry. WBM is preferably used, because it is known to be more environmental friendly compared to OBM. Another benefit is that recycling costs of WBM are significantly lower than of OBM. Nevertheless, WBM is also known for being not an optimal lubricator in the wellbore, presented by the typical friction factors in table 2.1.

The mixed water base fluid contains 5 weight % bentonite to provide the fluid with the necessary thixotropic properties. The added amount of barite is required to achieve a fluid density between 1,26 - 1,28 $\frac{g}{cm^3}$. For the MCR tribology measurements, a fluid with with additional 0,02 weight % hydroxyethylcellulose (HEC) polymer is prepared to increase the viscosity. Testing both fluids allows to observe a possible interaction between polymers and nanoparticles.

The first step is to mix the water with the bentonite. While mixing the brine, the bentonite suspended water is rested for at least half an hour before adding other components to the fluid. It allows a complete hydration of the bentonite, which could be inhibited by other particles. If the base fluid shall contain polymers, they are added and mixed to the brine in this step. To determine the amount of barite, a density measurement is done to calculate the necessary value. Every mixing is done for at least five minutes to ensure well dispersed fluid components. At last nanoparticles are added to the fluid, accroding to their weight percentage. The ultrasonic mixing apparatus, shown in figure 4.1, ensures a well deflocculated fluid. The ultrasonic fluid mixing is done for five minutes.

The fluid composition receives no further variation and additional components. The bentonite clay particles are sensitive to elevated temperatures. Therefore to maintain sample comparability, the fluid composition has been kept as simple as possible. Every fresh mixed fluid is used on the same day. This shall eliminate the aging process of fluids as possible error source.

4.2 Nanoparticles

The nanoparticles are selected according to the experience of industries, where they have already been utilized as friction reducers. They have not been introduced by the oil industry before for that purpose. In this experimental series it is distinguished between compact and fumed nanoparticles. Fumed nanoparticles will be the type of particles being tested. Well known lubrication materials are silica, titania and alumina, which are also available for the experiments. Titania and alumina are manufactured by Evonik Industries with the label Aerosil®. The particle size ranges from $40\,nm$ to

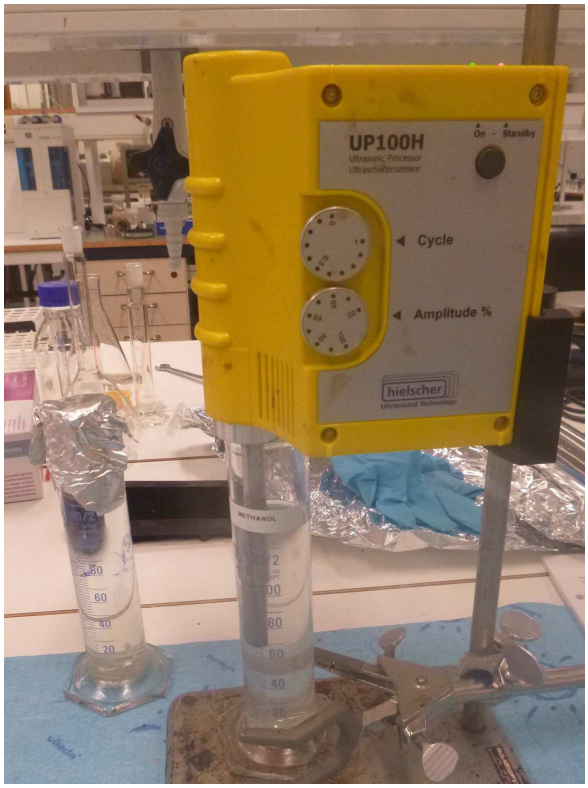

Figure 4.1: An ultrasonic mixing apparatus

$60\,nm$. Titania is a hydrophilic fumed nanoparticle sold as Aerosil® TiO_2 PF 2. It has a specific surface area of $57 \pm 12.5\,m^2/g$ and a pH value between $3.5 - 4.5$ in $4\,\%$ dispersion. [6]

Alumina (Aerosil® Alu 65) has also an average particle size of $40\,nm$ to $60\,nm$. It is a fumed metal oxide, with a specific surface area of $65 \pm 10\,m^2/g$ and a pH value between 4.5 and 6.0 in $4\,\%$ dispersion. [4]

The silica nanoparticles Elkem NanoSilica® 999 are compact particles from the company Elkem Silicon Materials. They have a mean particle size of $40\,nm$ and a specific surface area of $50\,m^2/g$ with a pH value of $3.0 - 5.0$. [3] [5]

During the testing process, the impact of nanoparticle size components within the drilling fluid shall be tested. Their effect on the lubrication properties of water based drilling fluids will be investigated.

4.3 Tribology and Rheology Testing Apparatus

The pin-on-disk apparatus and the MCR - tribology measurement method are the used instruments in the experimental phase of this thesis project for observing the lubrication effects of nanoparticles in drilling fluids. In this section, both apparatus are introduced to allow the reader an adequate traceability and to demonstrate the conditions of the tests.

The rheology measurement is done with the MCR viscometer cell application and detailed explanation about the handling and sample treatment is included.

4.3.1 Pin-on-Disk Apparatus

The pin-on-disk apparatus available in the Nanomechanical Lab at NTNU is shown in figure 4.2. Being able to test the drilling fluids with a pin-on-disk apparatus is excellent, since the test is easily reproducible. A disadvantage is that the tests are quite expensive.

The apparatus allows temperature specific measurements by heating up the lubricants with a heating spiral. The heating spiral is fixed into the disk and the sample holder.

First of all, the apparatus has to be cleaned appropriate by the user in order to begin with the sample placement, which includes the disk, the sample holding equipment, including the screws (see figure 4.3), the material samples and the pin with the steel ball. All parts have to receive an ultrasonic ethanol bath for at least five minutes. This removes all surface contaminations, and as many as possible small scale particles left from the previous experiments. After the ultrasonic bath all equipment will be dried under high air pressure to ensure that all remaining water is removed.

Then the material sample is installed onto the rotating disk cylinder with three screws. The material sample dimensions are $2.5 \times 2.5 \times 0.5\,cm$ to fit right under the sample fixation. The material type being tested is a typical casing steel: $ST\ 57$. This step is followed by the pin preparation. The steel ball is entered in the hollow cylinder and fixed with a pin screw on the other end, see figure 4.4. The steel ball material type for all experiments is a stainless steel AISI 316 of grade 100. The ball has a diameter of $6\,mm$.

The heating spiral is adjusted and mounted to the disk equipment. Thereafter the arm of the pin holder has to be calibrated into a horizontal level prior to the testing, illustrated in figure 4.3. This has the purpose that no inclination of the pin manipulates the testing result and the applied normal load is effectively transferred

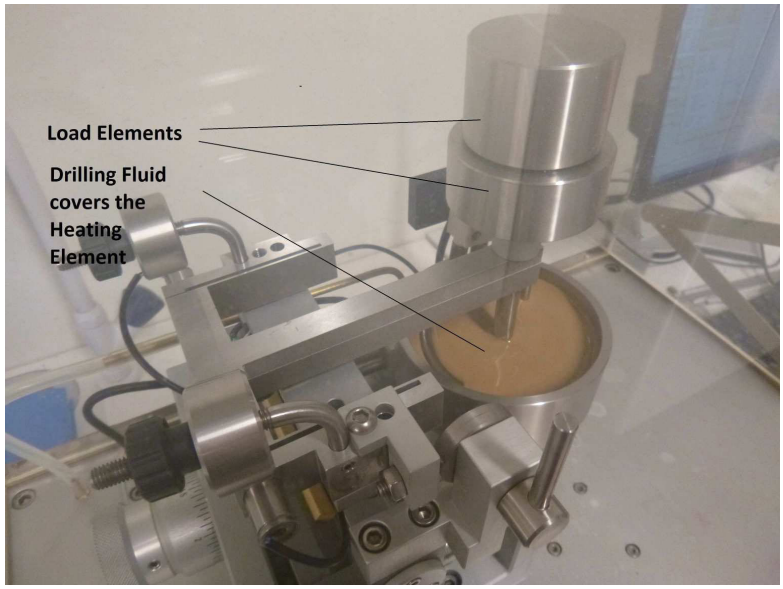

Figure 4.2: Pin-on-Disk apparatus

to the material surface. The pin arm is not in horizontal position for the further sample preparation and is left in an inclined position until all steps are done.

Afterwards, the fluid sample can be filled in the cylinder basin. The parameters for the testing row can be set up in the software program. The parameters for this test series will be a pin radius of $5\,mm$ with $120\,rpm$. With $2\,\frac{cycles}{second}$ the testing will last for 15 minutes, which means $1200\,cycles$ for each test.

The required fluid volume is approximately $100\,ml$, but it should be ensured that the heating spiral is completely covered with the fluid, since water based fluid will be used and the high temperature exposure to the fluid for minimum of 30 minutes might lead to a dehydration. The normal force is set to $10\,N$ for all experiments.

The temperature being used for the pin-on-disk apparatus is 50°C for each experiment. A higher temperature is not recommended, since the exposure time would lead to a higher dehydration which has a large impact on the fluid behavior. A too dehydrated fluid will not result in a representative value. A lower temperature is not used, because it will not represent the temperature range of the borehole. Before every experiment is started the room temperature and the room humidity has to be entered into the software system. When the previous mentioned steps are completed and the correct sample temperature is typed into the software, the preheating of the fluid sample can start. Depending on the temperature, this procedure will take up

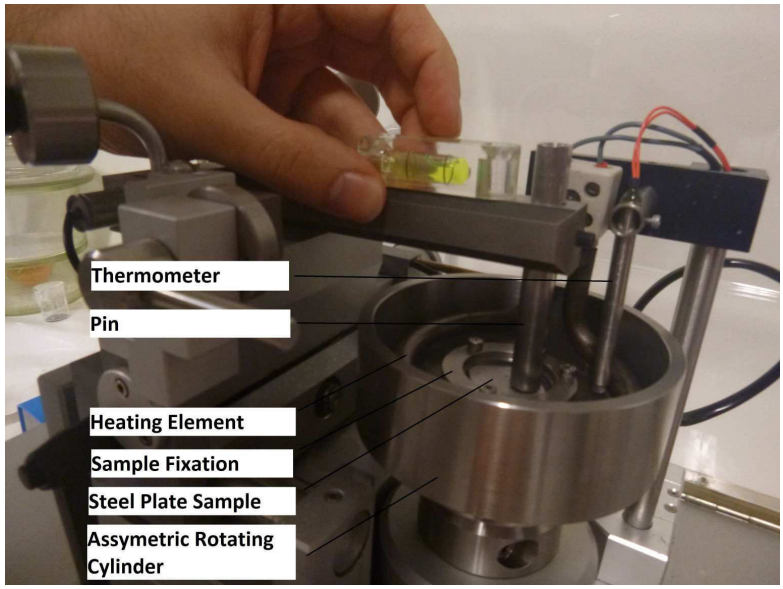

Figure 4.3: Sample Preparation for the Pin-on-Disk Apparatus

to 15 minutes. During this process the disk is in constant rotation mode, to ensure a constant temperature distribution and it keeps the fluid sample in constant motion.

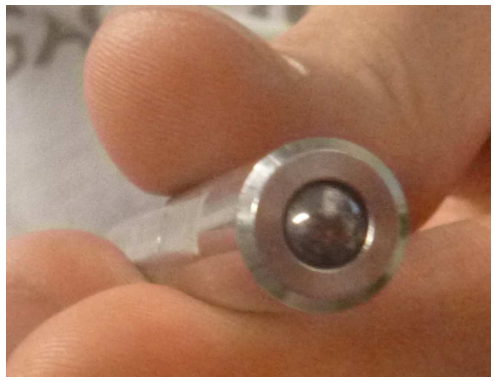

Figure 4.4: Illustration of the pin with a ball mounted to the bottom

As soon as the desired temperature is reached, the pin arm is lowered down to the sample material in the disk. To keep the arm in the horizontal position the normal force load will be added directly on top of the pin. Now the experiment is ready to start. Every experiment aims to finish the cycling without any interruption, jamming and noise disturbance. If any of these mentioned cases happens, the test

results are degraded. [13]

When the experiment completed successfully the cycles, the material sample and/or the ball is extracted for microscopic observations. An analysis gives more material specific information about lubrication efficiency of the nanoparticle being used. Knowing more about the failure time of the material could allow a conclusion about the practicability in the field. During the microscopic observations, the inner and outer radius of the wear track can be analyzed and measured. The 3D microscope also allows a profile picture of the track. The depth and width provide data for the equations listed in section 3.1.1 to calculate the volume loss of the material samples. [13] More information about the methodology and procedures can be read in the international standardization manual ASTM G99. [12]

4.3.2 MCR - Tribology Measurements

The first step is to prepare the apparatus by setting up every part of the equipment correctly. The correct tribometer measurement cell has to be installed to the MCR and the cooling system has to be switched on. In this case, the cooling supply is provided simply by a hose connected to the tap water.

All experiments shall be exposed to the same conditions, therefore it was decided to run most experiments at 25°C. It allows the same temperature conditions for all experiments, independent from the actual room and outside temperature. Sporadic tests with different temperatures of 50°C and 75°C are performed to see the influence of temperature on the lubrication behavior. Testing the fluid samples with higher temperatures than 75°C is not recommended, since the fluid sample of $2\,ml$ dehydrates quite quickly and the lubrication behavior will be strongly affected by this. The steel ball adjusts to room temperature and will impact the sample temperature as soon as it digs into the fluid sample. Out of this reason a predefined time of 2 minutes will be counted down before the testing starts to ensure temperature equilibrium.

The steel ball diameter is always $12.5\,mm$ and is pushed into the shaft of the pin. If the wear track allows it, the steel ball is used three times, whereat the ball is rotated after each test. This provides a new side of the ball without wear track. The material used for the experiments is for both the ball and the plates stainless steel 316 SS. The distance d between the spherical zenith and the contact point for each experiment is $1.0\,mm$.

All testing equipment and samples are treated with methanol in advance of each test to ensure clean surfaces and the removal of surface pollution. At all times latex gloves were worn to prevent contaminations. It was decided to run the experiments on the base of the Stribeck curve, which means an increasing rotational speed of the ball acting on the plates. The speed distribution during the tests is the same as

for the standard viscometer test: $3, 6, 100, 200, 300$ and $600\,rpm$. In table 4.1, the equivalent shear rate to each RPM value is written. The range was chosen to cover a big spectrum of possible real time data and to allow certain comparability. Each speed range is performed for 5 minutes in series nonstop, without any disturbance during the testing process.

The instrument is heated up to the defined measurement temperature and thereafter the fluid is added to the basin. The required fluid sample is $2\,ml$. A protection cap is laid on the fluid sample holder for safety reasons. Figure 4.5 shows the completed sample preparation stage just before lowering the ball shaft into the sample holder. While lowering the steel ball down to the fluid, the sample fluid has time to adjust to the desired temperature. The normal force F_N is $10\,N$ for each experiment. With the given angle α of the metal plates, the normal load, which is perpendicular to the plate surface, is automatically calculated by the software of the MCR according to formula 3.4.

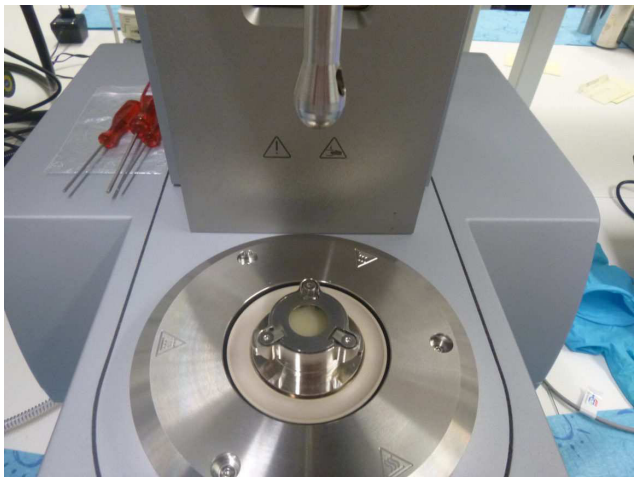

Figure 4.5: Fluid sample before testing the lubrication behavior

The apparatus and sample treatment remains the same for every experiment. It is up to the results of the experiments if more than two series of the same sample will be tested.

4.3.3 MCR - Viscometer

The Anton Paar rheometer in the laboratory of the Department for Petroleum Engineering and Applied Geophysics allows a variety of different measurements of the fluid behavior. A viscometer measurement cell can be installed onto the rheometer. Additionally to these benefits, the MCR viscometer allows a regulation of the surrounding temperature. An equal temperature for all experiments allows a better comparability between the samples. Higher testing temperatures allow more detailed fluid behavior description regarding the practical application.

For the laboratory testing, it was decided to use the MCR viscometer, which is more comfortable in use compared to the Fann viscometer. With the provided software of this apparatus, all parameters are set before the testing and visual impreciseness and manual inertia are avoided. The methology of the experiments are as following. The bob with cone is embedded in a cylindrical basin filled with drilling fluid. The measurement tool allows distinguishing between WBM and OBM by using the bob with cone or simply a cylindrical bob, see figure 3.4. For WBM the bob with cone is recommended to use, because it prevents the abrasion of the measurement tool due to the particle sizes in WBM. Both bob types have axial grooves along the surface, which prevents wall slip at high rotational speeds. The cylinder is shown in figure 4.6.

By applying shear force due to a defined rotation of the cone, the shear thinning behavior is observed. The shear force sequence is supposed to be the same as with the conventional Fann viscometer. It allows the comparability with other measurements done in the industry. All samples are measured at 25°C. Sporadic measurements are done at 50°C and 75°C to observe temperature coupling effects with the nanoparticles. Since rheology is temperature depended, a precise analysis of the behavior of the fluid can be done. Like mentioned in the previous section, a higher temperature is not used, since dehydration effect might negatively influence the measurements. The fluid sample in the cylindrical basin is approximately $10\,ml$ for each test.

The testing procedure starts with cleaning the equipment with water to remove the previously used fluid and second with methanol to clean the small scale contamination of the equipment. The software was set up with the temperature and the experimental speed ramp of $3, 6, 100, 200, 300$ and $600\,rpm$. Each speed interval was applying the same shear rate to the drilling fluid as the Fann viscometer does. The shear rates are listed in table 4.1. The cup has a mark inside, which indicates the required fluid volume. The sample fluid is filled into the cup and the preheating starts. When the fluid temperature is equalized, the bob is lowered into the cup until the tip of the cone has a $1\,mm$ distance to the cup bottom. A waiting time of 3 minutes and a visual control check with the electronically thermometer allows a temperature equalization with the fluid sample. Thereafter the sample testing starts with the

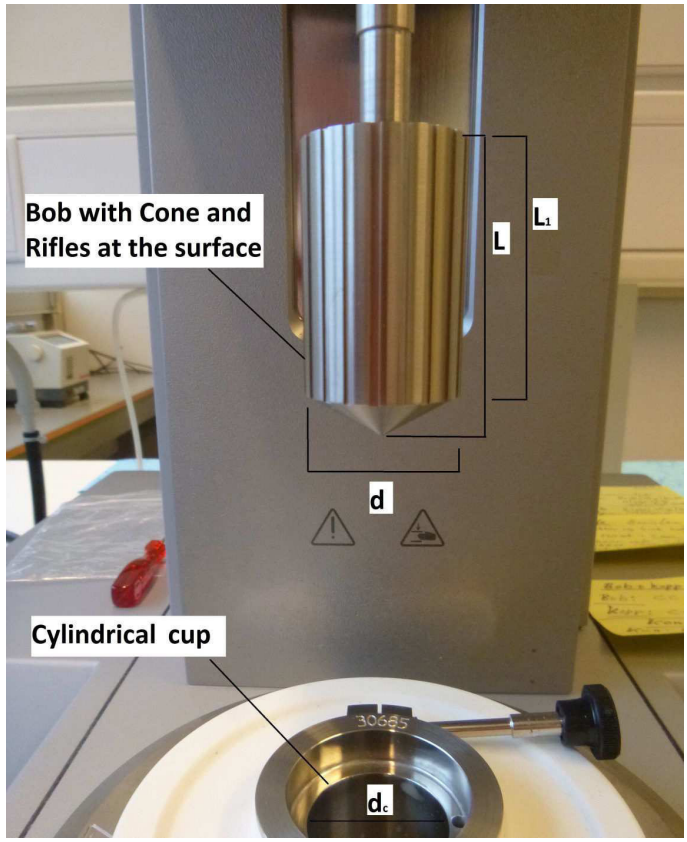

Figure 4.6: Concentric cylinder measurement with the MCR 302 SmartPave apparatus

speed ramp and one measurement point will be taken for each speed ramp right after the rotational speed is inclined.

The precise dimensions of the viscometer equipment are a total bob length (L) of 4.8 cm, where the cylindrical part with the axial grooves (L_1) of the bob is 4 cm long and the total diameter of the bob (d) is 2.65 cm. The inner diameter of the cup is 2.9 cm, which result in a ratio of 1.09, according to equation 3.10.

Table 4.1: Oil industry standard values for viscometer measurements

RPM	**Shear rate** $\dot{\gamma}[\frac{1}{s}]$
3	5,1
6	10,2
100	170
200	340
300	510
600	1020

Chapter 5
Results

In this chapter, the major results of the experimental phase are presented. First the MCR measurements are performed to find out the most useful temperature range and an optimal nanoparticle concentration in the water based fluid. The water based fluid contains barite, bentonite and HEC polymer as well as another series of water based fluid containing only barite and bentonite. With the results of the MCR apparatus, the pin-on-disk test series has been planned.

Most of the experiments generated a big amount of raw data. A relatively small amount is summed up in the appendices. The complete data set is copied to a CD attached to the thesis. The processed data and graphical illustrations are shown and presented as following.

5.1 MCR - Tribology Measurements

The laboratory tests with the MCR tribology cell are done prior to the pin-on-disk measurements, since the tests are cheaper and allow a higher number of experiments. The testing fluids consists of both water based fluid containing barite and bentonite and water based fluid containing barite, bentonite and additionally polymers. To each one of the base fluids the nanoparticles were added and tested at different temperatures.

The base fluid was either added with alumina, silica or titania nanoparticles. The average friction factors for each sample with its temperature conditions are listed in appendix B. One test series took 30 minutes, which was divided into six speed intervals to each five minutes. Each speed interval recorded 100 measurement points. The average value for each interval is stated in the tables listed in Appendix B. The mean friction factor value for each test series is also listed in these tables. Comparing barite, bentonite (BB) and barite, bentonite and polymer (BBP) based fluids with each other, the BB based fluid has a slightly lower friction factor than the BBP fluids at most of the low sliding speeds, seen in table: A.1 and A.2.

The other illustrated curves represent samples with containing nanoparticle fluids. These are generally characterized by an increased mean friction factor. The highest friction factor of 0.494 is recorded with 0.5 weight% titania based BBP fluid, table A.19. Whereas the mean friction factor values vary between 0.390 to 0.450 for the other cases.

To visualize the results, a graphical solution shall give an overview of the data. All reference points are colored blue. All fluids with a concentration of 0.1 weight%, 0.25 weight%, 0.5 weight%, 0.75 weight% and 1.0 weight% are colored green, red, black, purple and orange accordingly. The first graph in figure 5.1 shows the friction factor of the data plotted over the particle concentration. The friction factor for alumina particles with 0.1 weight% at 50°C and 0.5 weight%, 0.75 weight% at 75°C are the only values lower than the ones for the reference fluids. At a concentration of 0.1 weight% at 25°C and with 0.25 weight% and a temperature of 75°C, the mean average value is similar or equal the reference values. All other results show an increasing trend of the friction factor values.

Observing the silica added fluids does not show better lubrication results compared to the lubrication behavior of alumina added fluids, seen in figure A.1. The friction factors are also by trend slightly higher than the reference values.

Generally, the same results can be observed with the titania added fluids shown in figure A.2, with the exception that at 50°C the lubrication behavior changes oppositely the general trend. For the titania added fluids has to be pointed out that

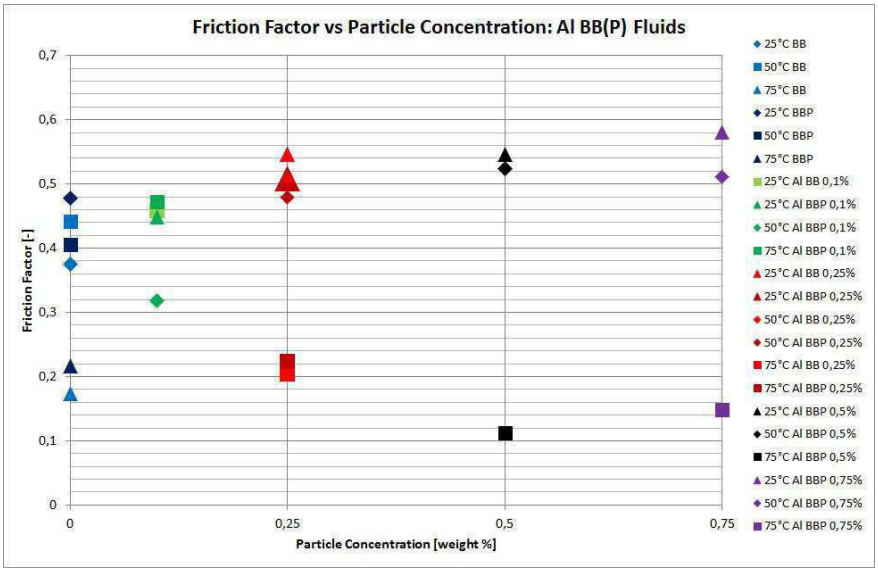

Figure 5.1: Friction Factor depending on the added particle concentration of alumina

the lubrication efficiency of the fluid increases significantly at a temperature of 50°C at both 0.25 weight% and 0.5 weight% particle concentration.

Regardless of the recorded friction factors, the amount of material wear seems to be independent from the friction factors. Figure 6.1 shows a comparison between 0.75 weight% added silica fluid tested at 75°C and a 0.1 weight% added alumina fluid tested at 25°C. According to the trend, it was expected that with increasing temperature, the friction factor will also increase. This is additionally supported by the fact that higher nanoparticle concentration would also result in a higher friction factor. But here although the particle concentration varies significantly from each other and the developed dehydration of the silica fluid is quite obviously seen on the picture shown in figure 5.2, similar friction factors are still recorded. One possible explanation for this phenomenon could be the formation of a smear film of the nanoparticles on top of the material surfaces, which protects the metal for further wear. At 75°C and with additional friction heat, the melding point of silica could be reached. A smear film formation with alumina particles at 25°C is quite doubtful. This effect could have resulted in a higher abrasive wear mechanism, here polishing wear that ended in a higher material wear based on the visual observation.

The recorded friction coefficient for each of the experiments is 0.47 (listed in appendix B in table A.8 and A.10).

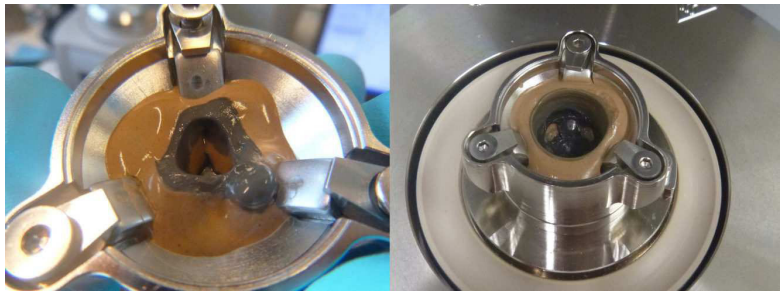

Figure 5.2: Fluid sample after testing the lubrication behavior. Left picture: sample test with 25°C; Right picture: sample test with 75°C

Figure 5.2 pictures two typical completed tests. The left picture shows a tested fluid sample at 25°C and the right picture shows a sample tested at 75°C. Both pictures visualize that the abrasive polishing wear mechanism during the testing phase is the more dominant wear mechanism. The fine particles observed during polishing can be seen in figure 5.2, because the test fluid turns dark gray. The illustrated pictures also show that the temperature significantly influences the sample rheology. The testing time of 30 minutes causes a high dehydration of the fluid and this results in a plastic deformation. The fluid is unable to flow back into the hole, which has been created by the rotating steel ball.

Since the temperature seems to affect the friction behavior, the figures 5.3, 5.4 and 5.5 illustrate the friction factor versa the temperature. The first graph in figure 5.3 visualizes the above mentioned results. Here the higher temperature of 75°C shows that the friction factor of 0.5 weight% and 0.75 weight% alumina added fluids is significantly reduced from 0.452 down to 0.357 and from 0.456 to 0.373 respectively, see table A.14 and A.15. With a particle concentration of 0.25 weight% a relatively constant friction factor can be observed, whereas a 0.1 weight% added fluid shows a significant increase in the friction factor from 50°C to 75°C. Both of the improved measurements are done with BBP fluids.

The next graph in figure 5.4 illustrates that all silica added fluids show by trend an increased friction behavior, but the collected data is not as extensive as with alumina added particles. With 25°C testing temperature more data was collected, but all data show a higher friction factor.

Similar result has been recorded for silica added fluids. For 0.1 weight% and 0.25 weight% silica concentration the friction factor is lower than the equivalent BBP fluid.

Likewise results are achieved with titania added fluids. All measurements result

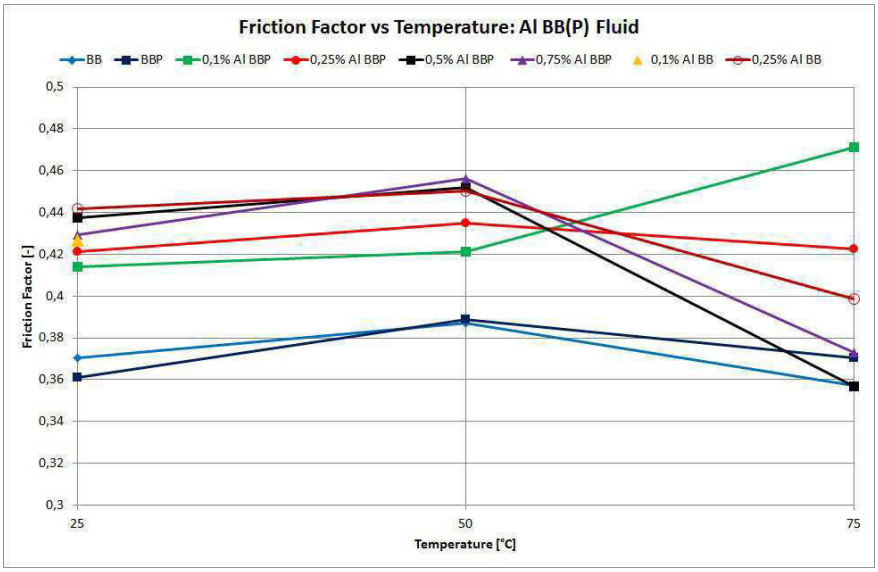

Figure 5.3: Friction Factor depending on temperature of alumina added BB fluid

in higher friction factors compared to the reference fluids. As an exceptional result, at 50°C a reduced friction behavior is recorded. There is an appreciable difference of the friction factor for the titania added fluid and the alumina added BB fluid which is higher compared to titania and alumina added BBP fluids.

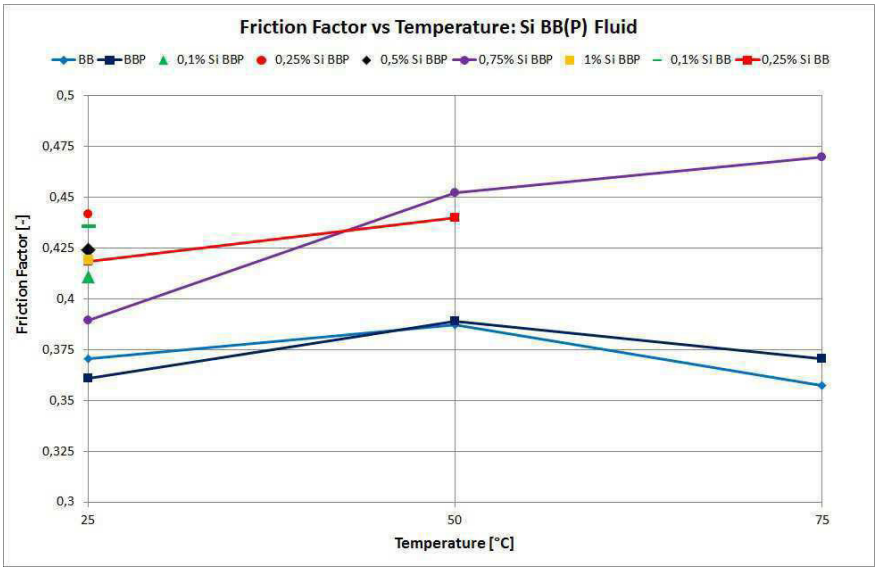

Figure 5.4: Friction Factor depending on temperature of silica added BB fluid

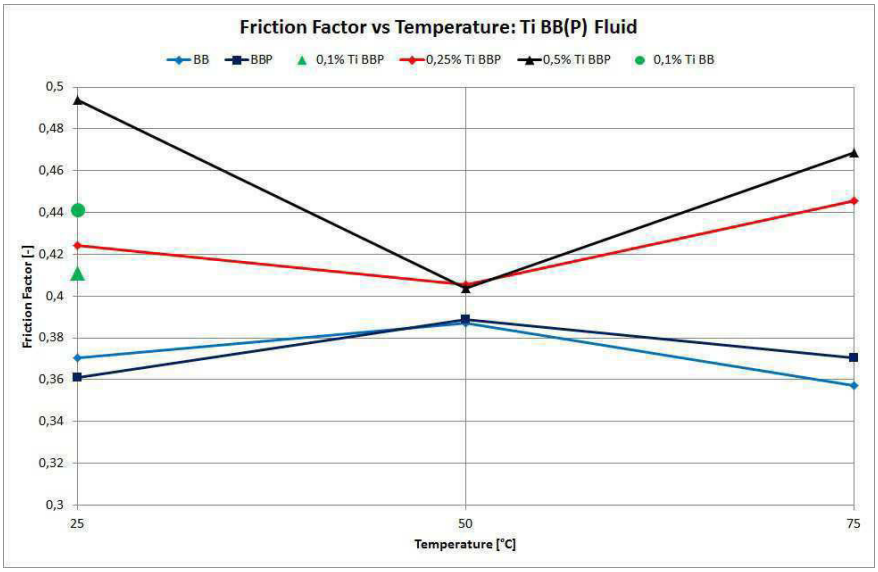

Figure 5.5: Friction Factor depending on temperature of titania added BB fluid

Another interesting point of illustration of the collected data is the friction factor development towards the sliding speed interval. Figure 5.6 illustrates the friction factors of the reference fluids. It shows that all tests have a similar friction curve. 25°C and 50°C tribology tests of BB and BBP end with lower friction factors at 600 rpm. The 75°C tested fluids start with a significant lower friction factor at 3 rpm and end with a slightly higher factor compared to the other temperature environments. By trend it is obvious that all tests show an increasing friction factor from 3 rpm to 6 rpm. The friction behavior seems to decrease from 6 rpm to 200 rpm and slightly increases again from 200 rpm to 600 rpm. Only the reference BBP fluid records a constant decreasing friction rate up to 100 rpm, followed by a constant friction rate to 200 rpm. From 200 rpm the friction behavior shows a slight increase. This is surprising, because 3 rpm and 6 rpm are nearby values, but have a significant different friction factor value. It could be possibly explained by an initial effect or homeogenized fluid or the temperature distribution in the fluid.

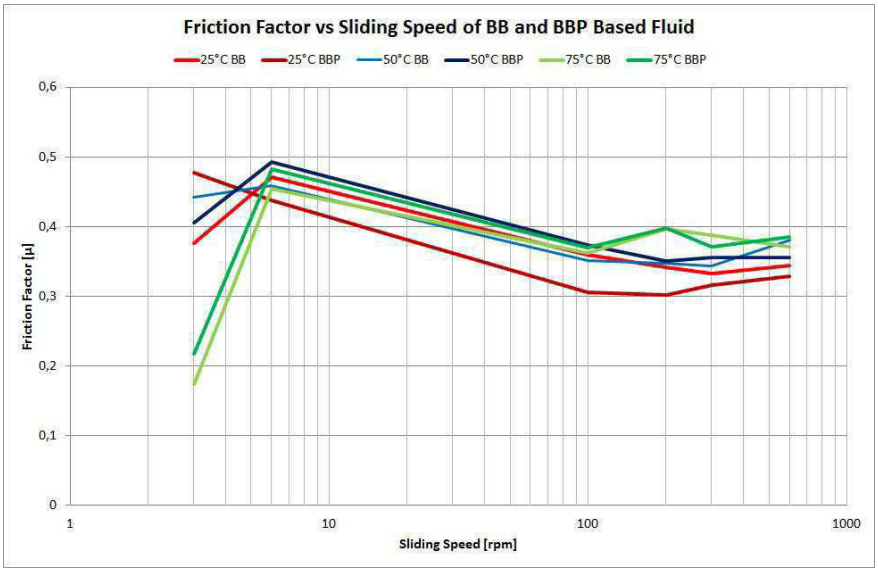

Figure 5.6: Friction Factor depending on sliding speed of BB(P) fluid

Since only the alumina added fluids show positive friction results at 75°C a closer look at the graph for friction behavior versa the sliding speed, illustrated in figure 5.7, is also of interest. The lower mean friction factor arises out of the lower sliding speed ranges from 3 rpm and 6 rpm. At 100 rpm the effect changes to the opposite and the mean friction factor is higher compared to the reference values. The trend of all curves is similar to the reference curves. This implies that the beneficial effect is valid only for slow rotational speeds and the total friction behavior is as adverse as the other nanoparticles samples.

The friction factors for the measurements of all silica added fluids at 25°C are presented in figure 5.8. No significantly lower friction factors are notable, except from the tribology curves for 0.25 weight%, 0.5 weight% and the BBP reference fluid. The 3 rpm value is higher, not lower as for 6 rpm, as mentioned previously. Possibly the 0.1 weight% concentration is not sufficient to behave differently from the reference value. And the 1.0 weight% concentration might indicate that possible nanoparticle effects might be counterproductive at such a high concentration of nanoparticle in the fluid. The friction behavior decreases down to 200 rpm and increases slightly up to 600 rpm again. Whereas the 0.1 weight%, 0.75 weight%, 1.0 weight% and BB reference fluid exhibit the same friction peak at 6 rpm.

The last graphical illustration shows the tribology curves of titania added fluid at 25°C. Here all curves show exactly the same flow behavior as the BB reference fluid. With increasing particle concentration the friction factor steadily increases.

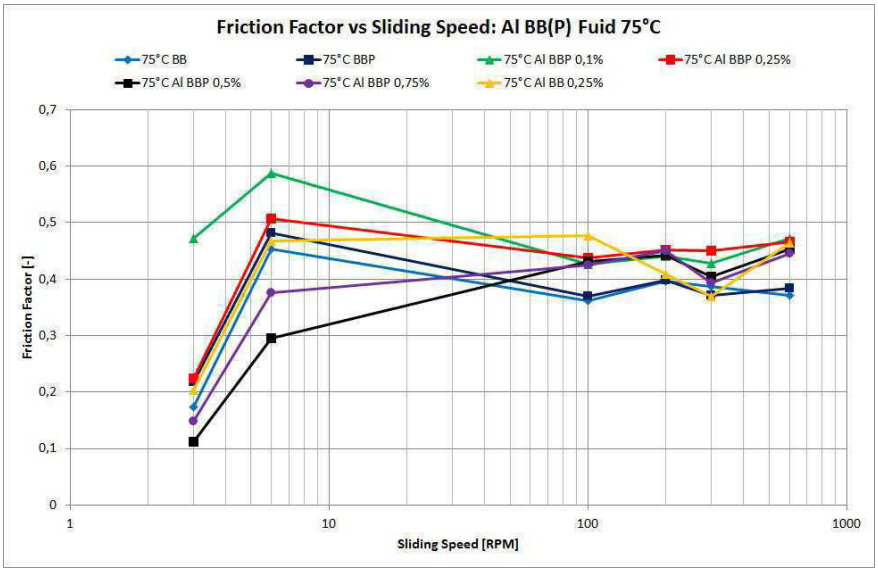

Figure 5.7: Friction Factor depending on sliding speed of alumina added BB(P) fluid, 75°C

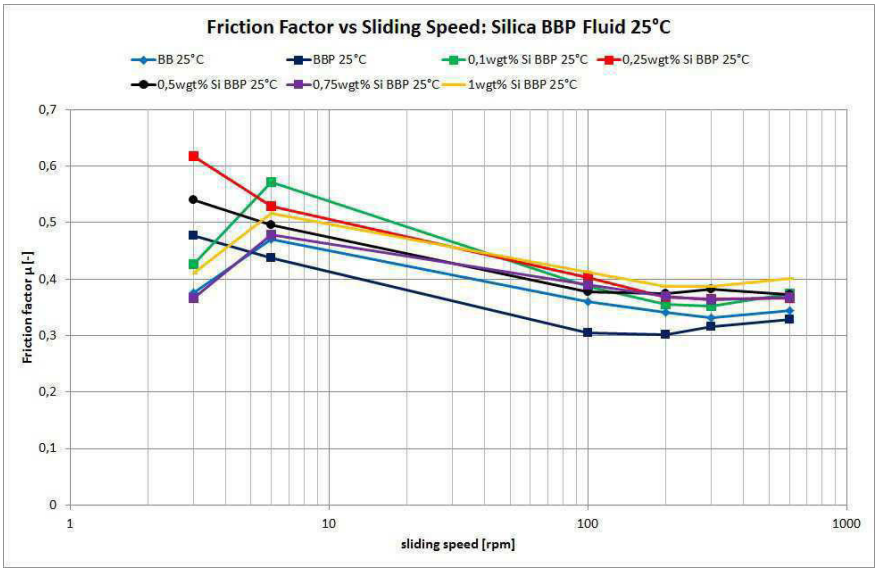

Figure 5.8: Friction Factor depending on temperature of silica added BB fluid

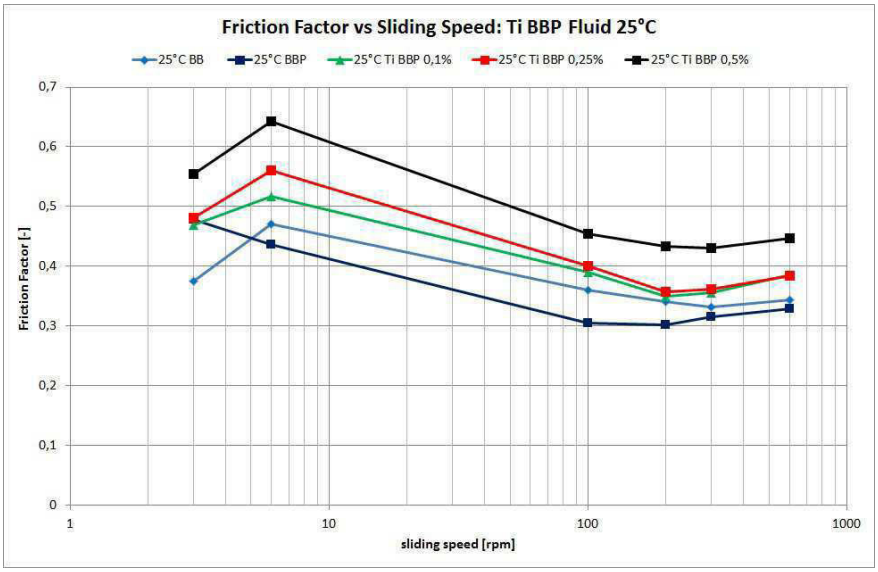

Figure 5.9: Friction Factor depending on temperature of titania added BB fluid

Sources of Error

The possible sources of error of the tribology test can be the changing room temperature humidity over the day, which cannot be influenced. The later the day and the more people are working in the laboratory, the more increases the room humidity. Especially, since the experiments are done at the end of the fall season, with many rainy days. Other days exhibited dropping temperature, which were characterized by cold and dry atmospheric conditions outside.

Another source aspect is that several tests are done with the same mixed fluid. Each experiment was very time consuming and even though the fluid was put in motion each time before a new sample was taken, the rheology properties could have changed over the time.

The fluid sample is quite small ($2\,ml$). The waiting time for reaching a temperature equilibrium after filling the sample into the basin could not have been optimal before the test started. The same issue might apply for the waiting time after the steel ball is entering the fluid sample.

In the tribology test, only a small amount of fluid samples has been tested and the lubrication fluids are viscous fluids, therefore the lubrication film between the steel ball and the steel plates may hardly be exchanged. With progressing testing time the lubrication film is more and more replaced by a mixture of small metal particles created from the material wear loss and the lubrication fluid. If this phenomenon is coupled with a high dehydration effect of the fluid, the reliability of the results might not be as accurate as supposed.

Regarding environmental/external impacts like building vibrations or other surrounding impacts, no influences were noticed. It has to be mentioned that all experiments were noisy starting from the 100 rpm rotational speed. With increasing speed the noise changed from a periodically squeaking to a continuous squealing.

5.2 Pin-on-Disk Measurements

A high degree of capacity utilization of the pin-on-disk apparatus requires a well-planned schedule on tests and their duration. Based on the results from the MCR - tribology measurements, it was decided to use only the barite, bentonite based fluid for further research testing at a temperature of 50°C. The pin-on-disk apparatus tests the lubrication behavior of only barite and bentonite based fluids. The other experiments differ by their amount of added nanoparticles like alumina, silica and titania with 0.1 - 0.5 weight% concentration. During the testing phase, the computer software recorded all friction factors, which occurred between the ball and the steel plate. Figure 5.10 illustrates the friction factor versus the testing time of three tests done with the BB based fluid. A third test was done, because the second test showed a larger deviation from the first results. The third test confirmed the test results from the first test and therefore the second test was considered invalid. Table 5.1 gives an overview of key data's recorded by the software. The minimum and maximum measured friction factor is measured during the entire testing phase, the mean value of all measured data and the standard deviation value.

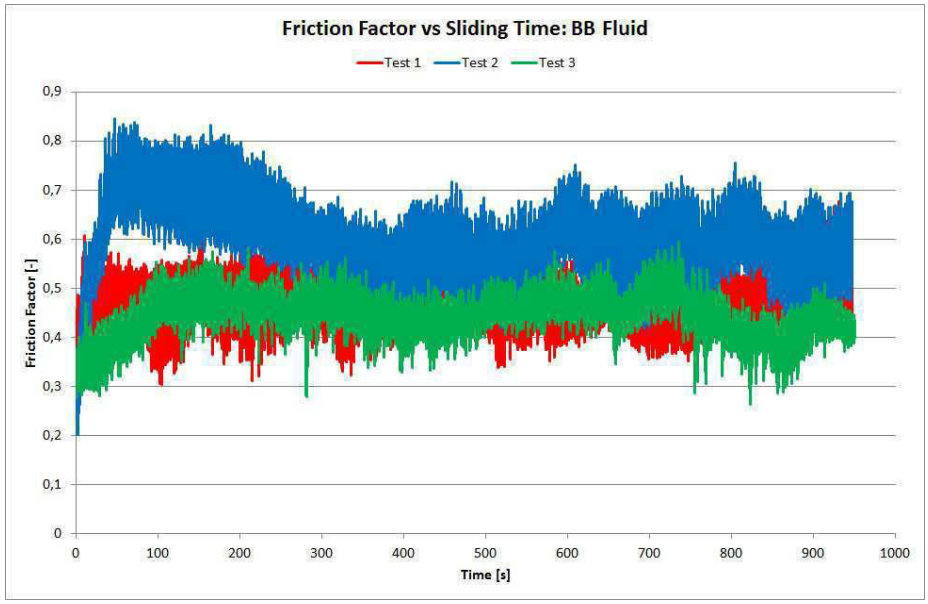

Figure 5.10: The friction factor of BB based fluid, 50°C

At least two experiments were done with the same type of sample fluid. As long as the mean friction factor value did not deviate more than ± 0.1 from each other, two experiments were assumed to present a repeatability and reliability of the experimental result. The fluid sample test which generated the lower mean friction

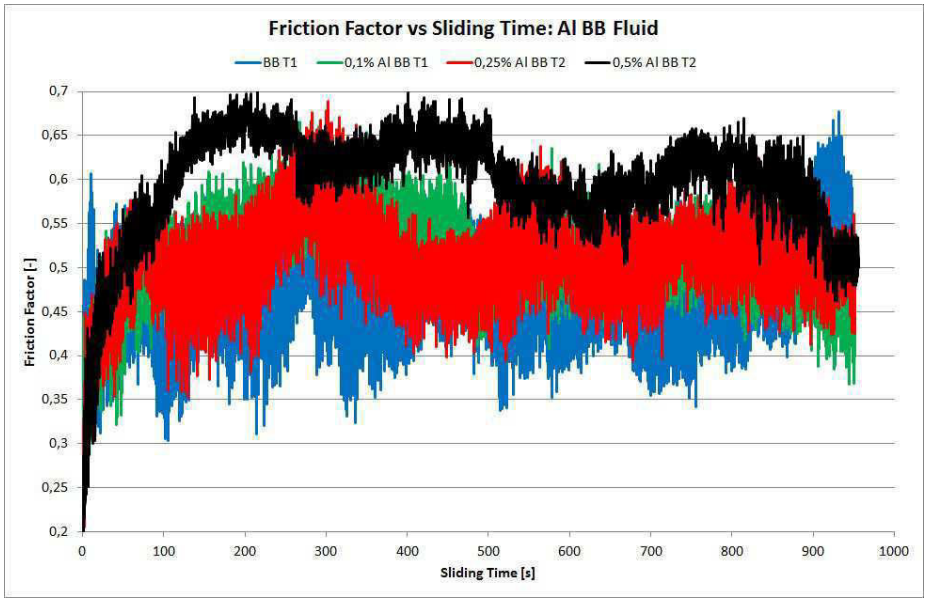

Figure 5.11: The friction factor of alumina added base fluid, 50°C

factors value was picked and is presented in the table 5.1. The mean friction factor value of BB based fluid is 0.570 and has a standard deviation of 0.128.

The friction factor of alumina added BB fluid with different nanoparticle concentration is shown in the graph of figure 5.11. All three concentrations are compared with the test results of the reference value of BB fluid, drawn with the blue color. Other colors in the graph are defined to 0.1 weight%, 0.25 weight% and 0.5 weight% to be green, red and black respectively. Here, it is not obvious that a concentration of 0.1 weight% and 0.25 weight% resulted in a reduced friction factor compared to the reference fluid, but the recorded raw values proved to be different. A particle concentration of 0.5 weight% alumina nanoparticles caused an increasing friction factor. The lowest mean friction factor is observed with 0.25 weight% alumina in the base fluid. The legend of the graphs states, which of the two performed test result caused the slightly lower mean friction factor value with the abbreviation T1 standing for test 1 or T2 for test 2.

The results of silica based BB fluid is different from the results of alumina. The graph in figure 5.12 shows that all the silica concentrations perform better than the reference BB fluid. The graph and the table 5.1 state that the best mean friction factor with 0.418 was achieved with a particle concentration of 0.25 weight% in the fluid. A lower and higher particle concentration result in a higher mean friction

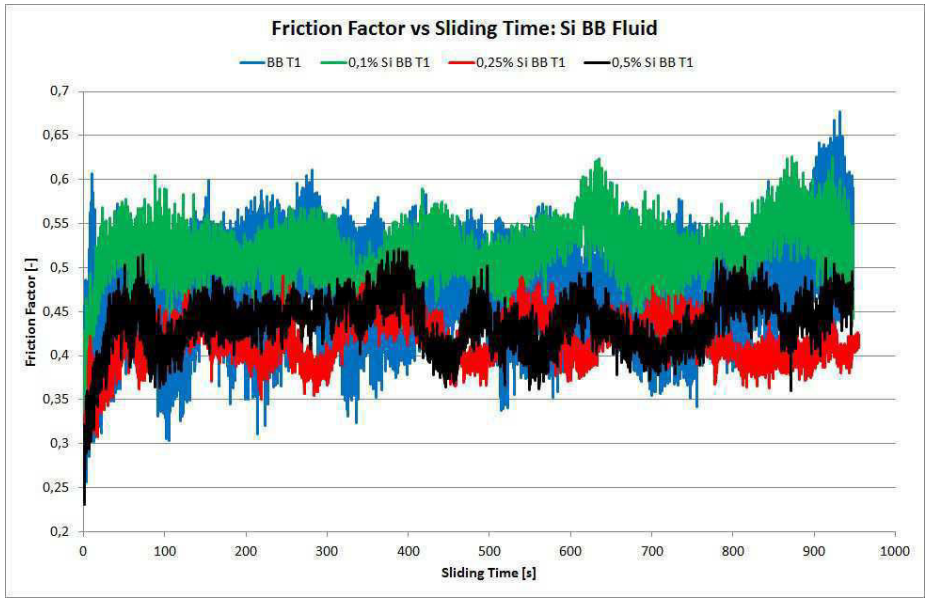

Figure 5.12: The friction factor of silica added base fluid, 50°C

factor.

Adding titania to the base fluid also results in lower mean friction factor values than the ones for the reference fluid. Here a constant decrease with increasing particle concentration can be observed, since the lowest mean friction factor for this testing series is achieved with 0.443 when the particle concentration was 0.5 weight%.

All told, the results of this instrument is that most (except alumina with a concentration of 0.5 weight%) nanoparticles added to the base mud result in a reduced friction factor. It is also interesting to see that all nanoparticle added fluids have a significantly lower standard deviation than the reference BB fluid. It seems like that the friction movement is smoothed out or less rugged with the nanoparticles as a component.

A successfully finished experiment results in a circular wear track for each sample material, as shown in figure 5.14. The wear track can be analyzed with the optical 3D confocal microscope provided by the Nanomechanical Lab, shown in figure B.1. The microscope is able to take layered pictures of the wear track. It gives detailed pictures of the surface asperity. For each sample the microscope took a picture of the sample and a cross line of the wear track is illustrated as a profile diagram. The cross line shown in figure B.4 is marked red on the picture. First, the reference test with the BB fluid was analyzed. Figure B.2 represents the wear track of the 0.5

weight% silica added BB fluid under microscope. The profile diagram of this test is shown on the picture below in figure B.3. The profile picture shows that the material asperity is already quite high, and that a clear profile of the wear track is difficult to define. Therefore the wear track dimensions are done visually by looking at the sample picture and by having a look at the profile diagram. The same procedure of taking pictures of the wear track and analyzing the profile diagram was done for all experiments. The figures and diagrams are attached in appendix A. All pictures taken by the microscope from the samples are included in the attached CD of the thesis. One wants to point out that for all wear track profiles with nanoparticle added fluids the profile is more obvious than the profile of the reference sample.

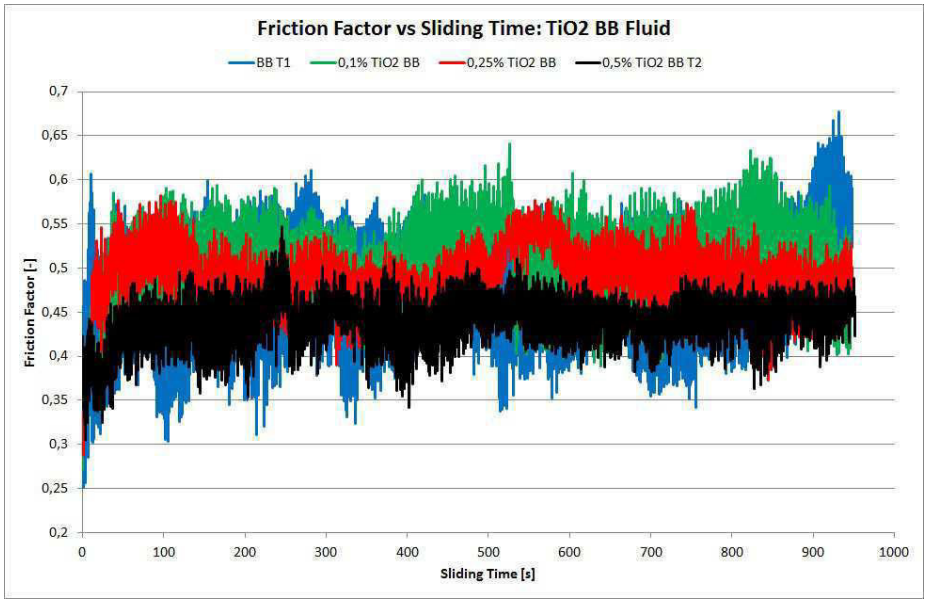

Figure 5.13: The friction factor of titania added base fluid, 50°C

According to the profile diagrams like in the figures B.3 and B.5, the volume loss for each sample can be calculated with the equation 3.3. Table 5.2 summarizes the data from the visual analyses from the microscope. The ratio of wear track width d_w to spherical radius of the impacting steel ball, assumed to be $0.5\,mm$, is of interest, when the material loss of the pin is negligible. As long as the ratio is $<$ 0.3 the calculated volume loss of the geometrical measurements is accurate up to 1.0 %. If the ratio is < 0.8 the accuracy of the result is up to 5 %. The ratio for all measurements varies between 0.371 for 0.5 weight% alumina added fluid to 1.130 for 0.25 weight% alumina added fluid. All ratios are above the 0.3 value and below the 0.8 (except the 0.25 weight% alumina added fluid). The test results exhibit an impreciseness of only 5 %, which is a rather good value. But on the other hand, the

two attached tables 5.1 and 5.2 allow a comparison between the recorded friction factors and the visually measured and calculated volume loss. It can be seen that there is hardly a relationship between these two values stated in the tables. Even though it is well known that there exists a correlation between these values. But the visual measurement is assumed to be very inaccurate, therefore the volume loss should not be taken as fixed. The calculated volume loss adds up to a 107.79 mm^3 for the reference fluid and, except of the 0.1 and 0.25 weight% added alumina fluids, all other nanoparticle added fluids result in a lower volume loss.

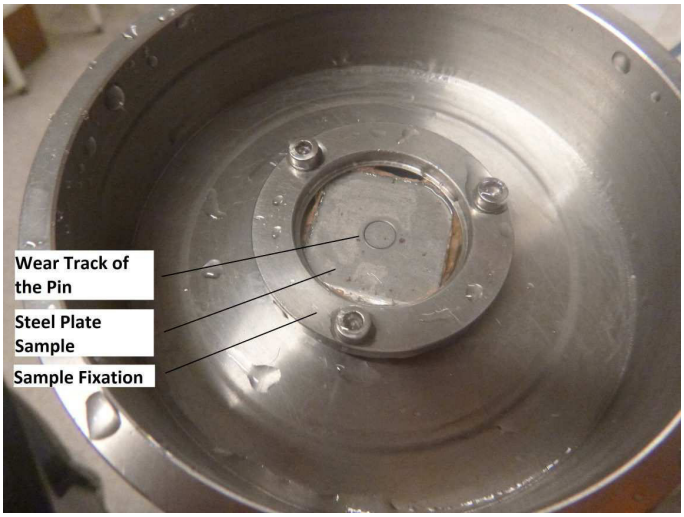

Figure 5.14: Circular wear track at the end of the experiment

Sources of Error

The cleaning of the entire equipment, which will be in contact with the drilling fluid, in ultrasonic bath shall assure a certain removal of fine dust and nanoparticles due to previous testing. However, in a practical environment it can hardly be fulfilled perfectly.

A source of error is the long exposure time of the fluid to the higher temperature of 50°C, where dehydration of the fluid might change the rheology of the fluid. Nevertheless, comparing the exposure time and the amount of fluid sample it can be assumed to neglect the dehydration. Working with water based lubricants is therefore quite sensitive. The entire apparatus is always covered up with a plastic cap during the heating up and testing phase. This creates a closed atmosphere with a high humidity environment. However, how large the change of the rheological behavior really is can be only predicted with uncertainty.

The testing time of 15 minutes is relatively short and visual wear observation might be difficult, since friction and wear is a time depended measurement. Developing wear grooves in the sample material requires a certain time, which was not given during these testing series. Therefore the large ratio of wear track width to the impacting spherical radius of the steel ball is relatively high. This can also lead to relatively high imprecision of the results.

The noise or external jamming effect is assumed to be nearly zero, no specific impacts occurs. No testing noises were noticed during the entire testing time and all experiments are successfully performed to the end.

Table 5.1: Friction coefficients of the nanoparticle added drilling fluids compared with the reference BB fluid.

Friction Factor	**Particle Type and Concentration** [*weight*%]									
	BB	**Alumina**			**Silica**			**Titania**		
	Fluid	**0.1**	**0.25**	**0.5**	**0.1**	**0.25**	**0.5**	**0.1**	**0.25**	**0.5**
Min	0.207	0.286	0.196	0.191	0.267	0.254	0.188	0.271	0.282	0.292
Max	0.864	0.684	0.691	0.706	0.638	0.501	0.532	0.641	0.591	0.547
Mean	0.570	0.521	0.514	0.599	0.517	0.418	0.438	0.503	0.492	0.443
STD	0.128	0.048	0.049	0.062	0.034	0.027	0.032	0.047	0.034	0.029

Table 5.2: Volume loss of the sample materials according to equation 3.3; d_w- wear track width, r_w-wear track radius

	Particle Type and Concentration $[weight\%]$									
	BB	**Alumina**			**Silica**			**Titania**		
	Fluid	**0.1**	**0.25**	**0.5**	**0.1**	**0.25**	**0.5**	**0.1**	**0.25**	**0.5**
$\frac{width}{sphere \cdot radius}$	0.659	0.778	1.130	0.371	0.608	0.505	0.428	0.546	0.386	0.553
$r_w[mm]$	5.16	5.19	5.28	5.09	5.15	5.13	5.11	5.14	5.10	5.14
$d_w[mm]$	0.33	0.39	0.56	0.19	0.30	0.25	0.21	0.27	0.19	0.28
$V_{loss}[mm^3]$	104.35	123.04	178.34	58.85	96.27	79.96	67.83	86.48	61.13	87.67

5.3 MCR - Viscometer Measurements

The viscosity measurements of the fluids give an idea, if the nanoparticles added to the base BB or BBP fluids influence the rheology. The first pictures in figure 5.15 illustrate results for one reference fluid, the BB fluid under different temperature condition. The temperature curves follow the Herschel-Bulkley model. With increasing temperature, the yield point of the fluid sample increases. The slope of the curve reflects the plastic viscosity and is lower for the flow curve with 50°C and 75°C testing temperature. The 50°C testing curve of the fluid has a higher yield point compared to the 25°C testing curve, but a lower shear stress at 1020 $\frac{1}{s}$. On the right picture of figure 5.15, the second reference fluid, the BBP based fluid is plotted. The increasing testing temperature shows also an increasing yield point shear stress. Compared with the BB reference mud, the slope of the 50°C BBP tested fluid has a higher inclination and has nearly the same shear stress at a shear rate of 1020 $\frac{1}{s}$ with the same fluid tested at 25°C. Notable is, that the flow behavior at 75°C of the BBP fluid has a dropping shear stress behavior to the shear rate of 170 $\frac{1}{s}$ and an increasing behavior until 1020 $\frac{1}{s}$.

The alumina component in both reference fluids increases the yield point. For both sample tests with BB and BBP based fluids, the flow curves show identical shear behavior at 25°C and 50°C. The plastic viscosity of 50°C BBP is less steep increasing than the 25°C tested fluid. The flow behavior is characterized with a high increasing shear stress from 3 rpm to 6 rpm shear rate. Thereafter, the decreasing shear stress ends in shear stress equilibrium. On the left picture of figure 5.16 the flow behavior of alumina BB fluid at 25°C and 50°C is presented in comparison with the 25°C BB fluid, colored in green. In addition, the right picture shows the tested fluid at 75°C testing condition. Here, the initial yield point shear stress is $88\,Pa$ high. For alumina fluid a nearly zero inclination of the flow curve is observed, which means a not changing flow behavior at different shear stresses.

The flow curves shown in figure 5.17 represent a 0.1 weight% and a 1.0 weight% silica added fluids. Both flow curves follow more the Herschel Bulkley model than the alumina added fluids. Other than the alumina added fluids, the silica added fluids do only slightly rise the initial yield point. As with the reference fluids the curve slope decreases with increasing testing temperatures. Abnormal curve behavior can be observed with the 75°C flow curves. The 0.1 weight% silica based fluid shows a variation of monotonic increase in the shear rate range of 10.2 - 510 $\frac{1}{s}$. The variation is not seen in the 75°C curve, but the sudden increase of shear stress from 3 rpm to 6 rpm can be observed, just like it can be seen with the alumina BBP based fluids.

Titania added BB fluids at 25°C with different particle concentrations are illustrated in figure 5.18 in comparison to the reference BB fluid. The flow behavior are

very similar to each other, whereat the titania added fluids show an increasing initial yield stress with increasing particle concentration. All fluid curves are more or less according to the Herschel Bulkley model. The initial yield point is similar high to the yield points of silica added BB fluid at 25°C.

In summary, nanoparticle added fluids have a higher initial yield stress and generally can be described with the Herschel Bulkley model, except the alumina added fluids. At high temperatures an abnormal flow curve behavior can be observed. According to Hiller et. al. (1963) [15], the plastic viscosity decreases with increasing temperature.

Contrary to Hillers theory, the yield point increases. This can be explained by a starting agglomeration of the drilling fluid. High plastic viscosity is usually an indicator for an excessive amount of colloidal particles in the fluid. [20]

Test Conditions

Testing conditions regarding the temperature impact of the sample include an additional error. The exposing temperature causes also for this experimental set up a certain dehydration to the fluid, which can have an influence on the rheology. The time between each sample testing has been set to 5 minutes, which might cause a further dehydration at higher temperatures.

Another aspect is the temperature adjustment of the MCR. When heating up the equipment the sample fluid with the cylindrical basin is not set into the machine yet. When entering the fluid sample into the machine the temperature decreased, but in a short period of time it was raised up again to the desired measurement temperature. However, the equipment thermometer measures only the steel surface temperature of the cylindrical basin, not of the fluid itself. This implies that during start of the tests the fluid temperature might be slightly different to the one stated. The fluid volume temperature gradient of $10\,ml$ is limited. Each test was repeated two or three times to ensure the reliability of the test.

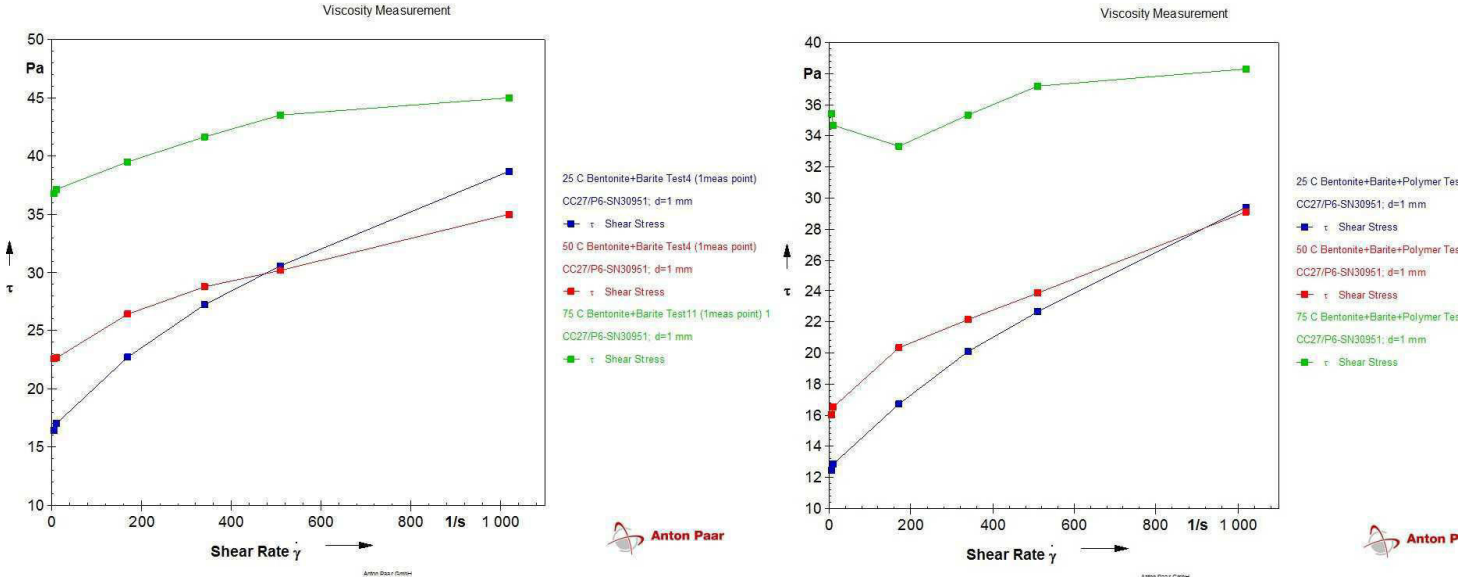

Figure 5.15: Left picture: Viscosity measurement of BB based fluid; Right Picture: Viscosity measurement of BBP based fluid under different temperature conditions

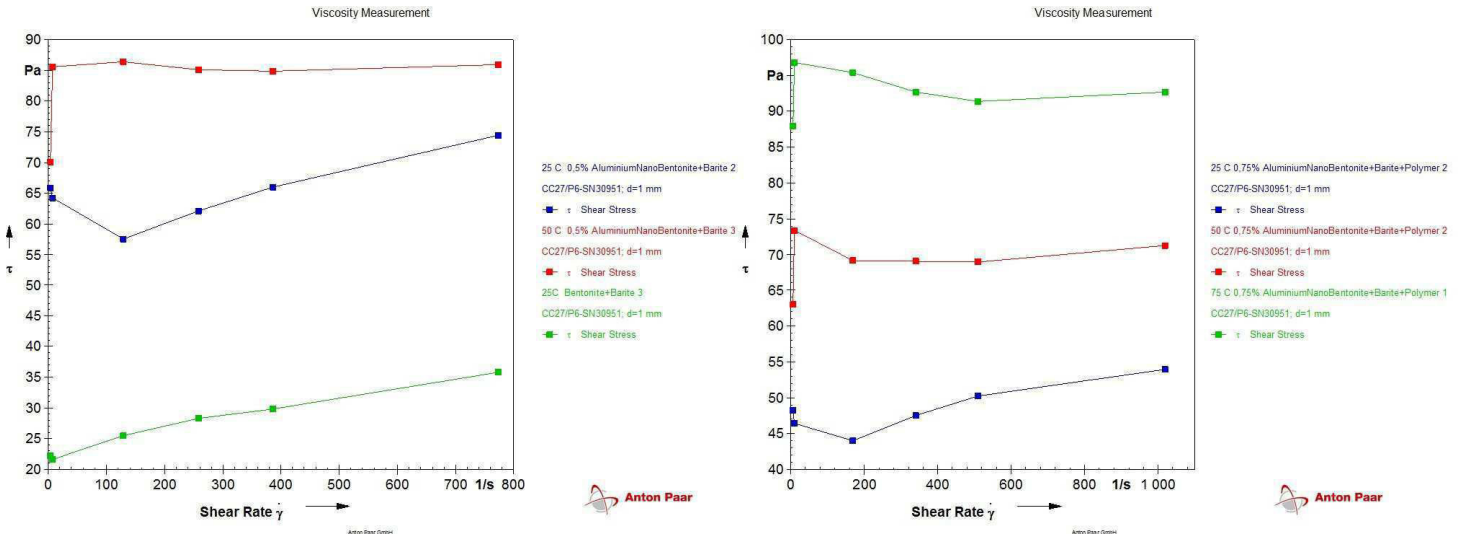

Figure 5.16: Left picture: Viscosity measurement of alumina BB fluid; Right Picture: Viscosity measurement of alumina BBP fluid under different temperature conditions

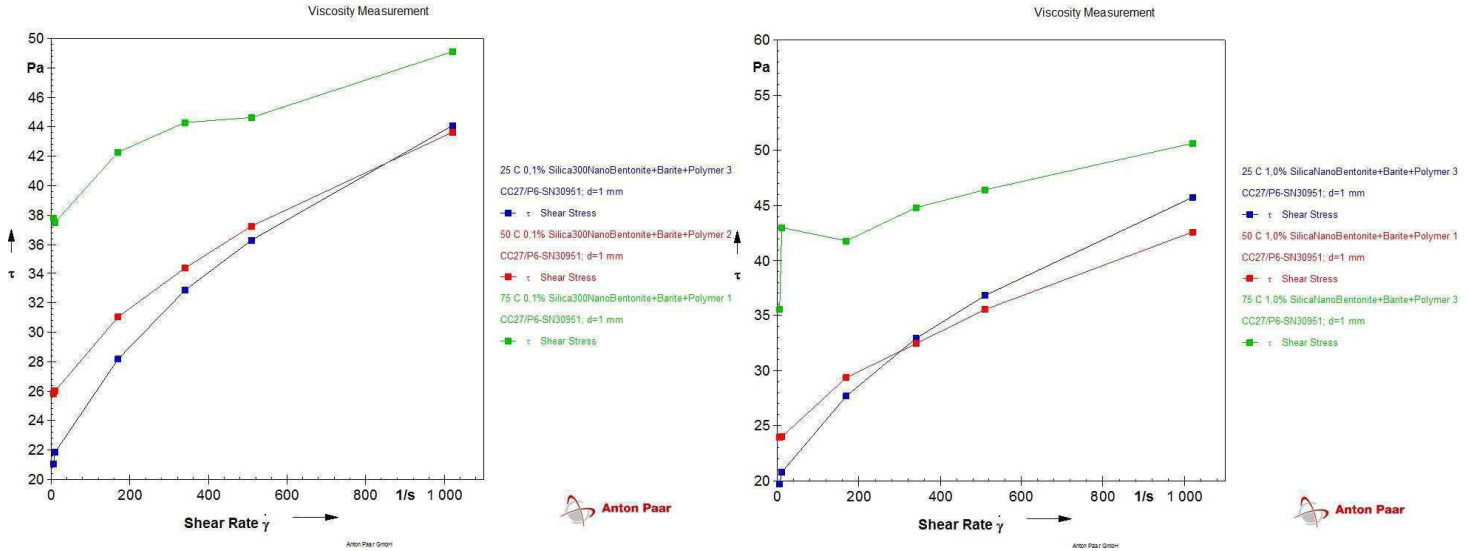

Figure 5.17: Left picture: Viscosity measurement of 0.1 weight% silica BBP fluid; Right Picture: Viscosity measurement of 1.0 weight% silica BBP fluid under different temperature conditions

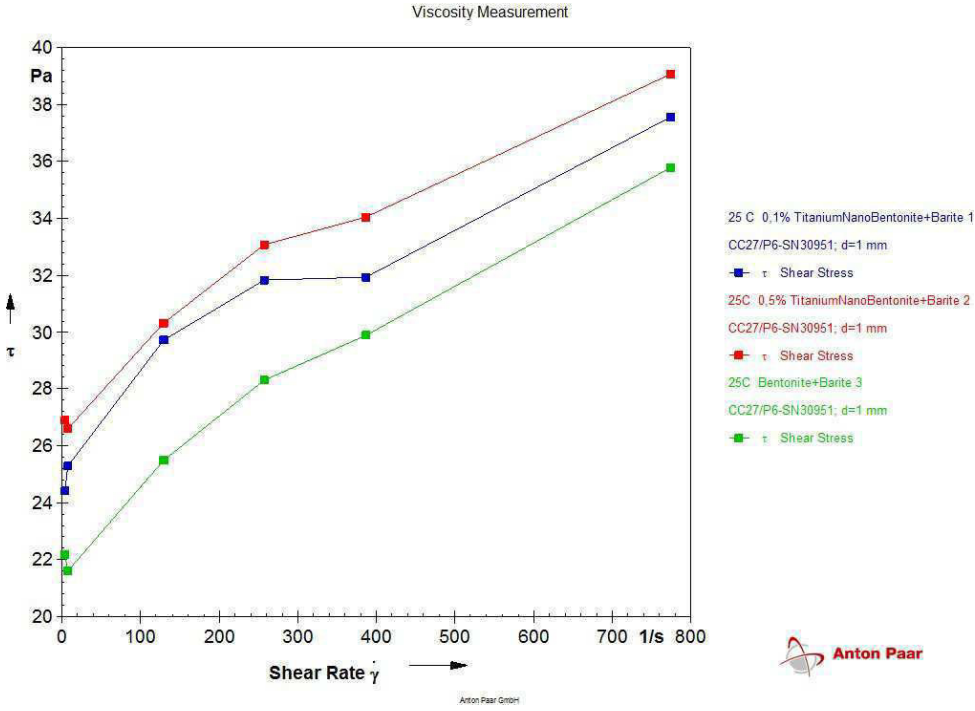

Figure 5.18: Viscosity measurement of 0.1 weight% and 0.5 weight% titania BB based fluid at 25°C

Chapter 6
Discussion

Two different experimental instruments were used to test the possible friction reduction of steel surfaces by using water nanoparticle based fluids. Both test apparatus result in different values.

The possibility to use the MCR tribology apparatus for preliminary experimental tests to the pin-on-disk apparatus allowed a vague preselection of possible testing fluids for the standardized pin-on-disk apparatus.

A vague preselection means the MCR tribology results appeared to be not as precise and meaningful as the pin-on-disk results. Other than the results for the pin-on-disk measurements, the lowest mean friction factors are achieved with the reference fluids, which are the BB based fluid and the BBP based fluid. According to these test results, no beneficial friction reduction would occur between two metal surfaces. A slight indication of temperature dependent friction behavior might have been provided by the alumina added fluid at 75°C where by trend the friction factor was reduced compared to the reference fluids. The fluid exchange capacity in the metal-metal contact area was very limited and the worn metal splinter contributed to an additional polishing wear mechanism. Other wear mechanisms had not obviously benn observed.

The visual comparison in figure 6.1 of the two different base muds with different nanoparticles and particle concentration show that even though the recorded MCR friction data is similar; the material differs from each other. In this case, either the high nanoparticle concentration of silica in combination with the high temperature of 75°C results this reduced wear or the alumina concentration at this low temperature causes higher abrasion. Both tests have BBP as their base composition and can therefore be compared.

Despite of the adverse friction behavior at higher temperature ranges in the MCR, it can be proven that there is a relationship between temperature and added

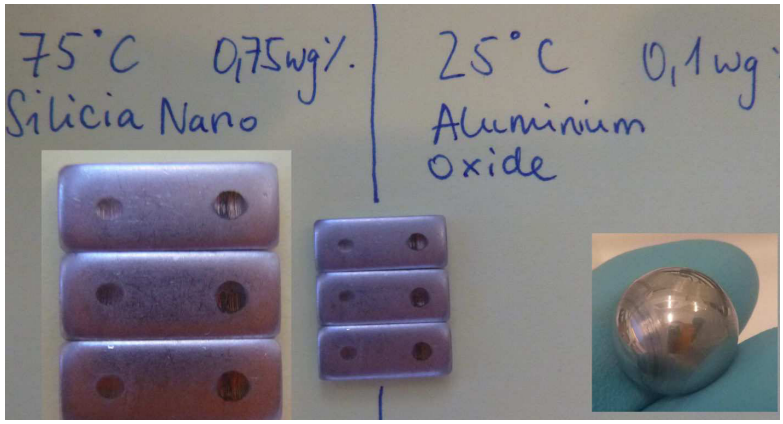

Figure 6.1: Different abrasioin wear at different temperatures and nanoparticle components; alumina BB fluid and silica BBP fluid

nanoparticles in the fluid. With the MCR tribology apparatus, the friction factor fluctuates with increasing temperatures also depending on the particle concentration in the fluid. While testing the alumina and titania added fluids in the MCR apparatus, the friction behavior is lowest for the titania fluid at 50°C. For the alumina fluid, 75°C is the most optimal temperature for this experiment. In contrast to these material and concentration specific coupling effects, a steady increase in the friction factor is observed with the silica added fluids.

Generally spoken, it can be said that an increasing fluid temperature causes a reduced viscosity of the fluid, but an evaporation of the water content from the fluid sample leads to an increase in viscosity on the other hand. The dehydration effect of the MCR measurement tool was relatively high at 75°C and it obverse impacts the temperature viscosity effect. But these parameters cannot be specified and clarified within this experimental test series.

The graphical illustration of the MCR data plots friction factor vs. concentration and friction factor vs. temperature. The diagrams are based on the mean value of the recorded total testing phase. Since the testing phase is divided into different speed intervals and the fluid sample might be more or less influence by dehydration and increasing amount of metal splinters in the testing fluid, the standard deviation of each speed interval varies. Especially at the beginning of the tests, a higher standard variation is usually observed than at the end of the experiment. One explanation is that each experiment requires a certain run-in phase of the metal to metal contact or that at lower sliding speeds the friction coefficient is generally higher than at high sliding speeds. This uncertainty cannot be further clarified within this range of experimental setup. To simplify the graphical illustration the average friction values

are plotted even though it includes a higher imprecision.

Out of this reason, the graphs which plot friction factor vs. sliding speed are plotted to show that there is a relationship between friction factors and the rotational speed.

Another effect to reduce wear is the chemical transformation of the particles to a smear film on top of the material surface. Even though the friction coefficient was recorded to be constant, the material wear differed significantly. This effect can only be appear at higher temperatures. But further investigations regarding the smear film was not done, since the observation of such a film is difficult and hard to realize.

The ball zenith to the bottom of the fluid basin is $1\,mm$ for all experiments. Most experiments were performed with a friction noise. This could have been probably prevented with a larger distance, but in our case the contact between the two materials could be ensured. An ideal placement adjustment has not been found out yet. One possible explanation for the friction noise can be that other bigger particles like barite could cause noise during the testing and influence the friction behavior. In that case the larger particles could act as third part particles abrasion wear, because the contact of the two materials is smaller than the barite particle sizes.

As a result of the MCR data, it was decided to continue with the BB fluid for the pin-on-disk instrument. No significant difference in friction behavior was observed between the BB and BBP reference fluids. Based on the Brownian motion theory and interparticle attraction, introduced in Section 2.3, the possible electrochemical and steric force impact of polymers towards fluid flocculation and agglomeration should be eliminated. Therefore further tests with the pin-on-disk apparatus were done only with BB based fluids. Additionally, polymers are much larger compared with nanoparticles and the possible ball bearing effect could be outbalanced by the characteristically stretching out effect at high shear stress situations. The possible third party abrasion wear does not play a role here, because the larger particles are able to draw aside when the higher impacting force passes by.

Another preselected parameter prior the pin-on-disk testing phase was the testing temperature. To be on the safe side, based on these testing experiences, the testing temperature for the pin-on-disk fluid was decided to be 50°C, for all tests. The pin-on-disk apparatus is also an open air testing instrument, which seems to be critical for long term tests and higher temperatures, because the base fluid is water. Testing the fluid with 50°C at 120 rpm sliding speed and surrounded by approximately 100 ml testing fluid may not provide a realistic temperature environment, but at least the rotational speed is a common drill sting rotation in the field. Realistic temperature environments depend strongly on the borehole depth, shown in figure 2.4, and are higher than 50°C. But this is also a limitation of WBM in reality, that

high temperature drilling is usually drilled with OBM, since the boiling temperature of the WBM is approximately 100°C, influenced by the fluid composition.

Considering the required fluid sample needed for the pin-on-disk experiments and the reduced wear testing time of 15 minutes, it could have been possible to test higher temperatures than 50°C without reaching a critical dehydration stage of the fluid, but the dehydration effect is herewith well eliminated and does not need to be considered. On the other hand it also allows the conclusion that the melting point temperature of all nanoparticle materials is not reached, which excludes the smear film theory stated in the semester project. It is assumed that all friction factor results are based on the mechanical effect of the fluid composition.

Comparing the results of the two instruments, the pin-on-disk apparatus recorded a beneficial friction coefficient reduction with nanoparticle based fluids. Especially silica added fluids show a significant friction factor with increasing particle concentration. Titania added fluids seem to be only beneficial up to a particle concentration of 0.25 weight% at 50°C, because the volume loss increases again with a particle concentration higher than 0.25 weight%. On the other side the friction coefficient values prove exact contrary results. In particular, with increasing particle concentration of titania in the fluid, the friction factor reduces, but with increasing silica concentration the friction factor increases again at a higher particle concentration than 0.25 weight%.

For alumina applies also a nonlinear relationship between friction factor and volume loss of the sample material. Based on these results, it can be summed up that there seems to be a link between friction and wear but it is not linear. Critically, it has to be mentioned that the visual measurements of the wear grooves succumb the uncertainty of the visual identification and definition of the wear track under the microscope. It can be possibly explained with the Mohs hardness of each material. The Mohs hardness of rutile is 6, the one for SiO_2 is 7 and for Al_2O_3 is 9. The significantly higher hardness for alumina my generate a higher wear.

Since no further tests were done with the pin-on-disk apparatus under different temperature conditions, more detailed conclusion about the temperature impact on the lubrication behavior of nanoparticles cannot be done. The materials being used are all fumed nanoparticles and are characterized by a mean particle size of approximately 40 nm. But each one of them has a different surface specific area, titania with $57 \pm 12.5\, m^2/g$, alumina with $65 \pm 10\, m^2/g$ and silica with $50\, m^2/g$. The surface to volume ratio allows a low concentration of the required nanoparticles in the fluid to achieve a beneficial effect. The slightly higher surface area of alumina perhaps explains the slightly higher friction factors during the pin-on-disk experiments. With increasing particle concentration the friction factor increased. Another explanation for the limited success of alumina as a friction reducer could be the material properties,

e.g. the load resistivity of the material. The highest possible normal load which can be applied on the apparatus proved that a friction reduction can be realized. That implies that the particle solidness can withstand such a high load without destroying the particle shape.

However, for detailed friction coefficient information it can be drawn the conclusion that the MCR tribology measurement tool is not suitable for this type of testing as it was done in this project. But the visual observation of the created wear in the MCR apparatus could give a bigger informational value than only the recorded friction data. Coming back to the visual observed wear with 0.75 weight% silica BBP fluid at 75°C and the 0.1 weight% alumina BBP fluid, this observation is proved by the pin-on-disk apparatus. Table 5.2 states that 0.1 weight% alumina causes 123.04 mm^3 volume loss, whereat the 0.5 weight% silica added fluid causes a volume loss of 67.83 mm^3. Since here the testing fluid is BB and the MCR observation was done with BBP fluid, it can be assumed that the impact of polymers with nanoparticles is not as significant as assumed at the beginning. Additionally, the visual observation was done with 0.75 weight% silica added fluid, which allows the conclusion that a further increasing particle concentration could be beneficial to the friction behavior. This is supported by the decreasing friction factor trend presented in table 5.2. Different than the MCR tribology experiment, the pin-on-disk apparatus was tested with a different material type, which corrodes. Therefore corrosion as another wear mechanism impacts the visual observation additionally. This is a significant source of error, which makes the results of the visual measurements quite unreliable.

To sum up, the results of the pin-on-disk apparatus are in agreement with the ball bearing effect theory. It was possible to prove friction reduction in WBM with nanoparticles as fluid components. Other previously published work mainly investigated the lubrication behavior of nanoparticles in combination with OBM and excluded tests with WBM. Even though the two used tribology instruments present different values, each one of them contributes to a nanoparticle temperature and particle concentration relationship. The standard deviation of nanoparticle added fluids reduces significantly, which makes all friction processes smoother and more stable. The lubrication efficiency depends on particle concentration in the base fluid.

The viscometer measurements provide clear data about the impact of nanoparticles towards the fluid rheology. An increasing concentration of nanoparticles results usually in an increase in the initial yield point of the fluid. This effect is reinforced by an increasing temperature environment. The effect varies between the material types of nanoparticles. This supports the coupling effect between temperature and the added nanoparticles to the fluid.

An increasing initial shear stress can be problematic in real borehole environments,

since it will have an impact during circulation stops. A higher shear stress has to be overcome in order to start again the fluid circulation. Pump limitations and narrow pressure windows are especially sensitive regarding a higher yield point. The ECD has to be carefully regulated in order to prevent formation fracturing at the bottom of the borehole. An interesting aspect could be that nanoparticles could act as viscosifier substitute and as friction reducer at the same time, which allows reducing the amount of other fluid components. Due to the fact that a small amount of nanoparticles is required to achieve the increased viscosity, the total particle volume fraction could be reduced. According to the Brownian motion theory, this will be beneficial to the electrochemical and antiparticle attraction between the particles itself and possibly reduce particle agglomeration.

Viscosity in reality is not only influenced by the physical, chemical and electrochemical processes of the fluid. Another impact is the interaction with the formation being drilled through. This was not put into further consideration in this project.

During the laboratory fluid mixing process, an ultrasonic mixer was used to ensure well dispersed fluid samples. Such a mixing procedure needs to be developed for practical well side applications, since with a well dispersed drilling fluid the drilling performance fluctuates.

To conclude, the theoretical potential of nanoparticles in drilling fluids is proven. With the experimental results of this project, the practical potential of nanoparticles in WBM acting as friction reducers could also be proven. It is of significant importance to find the suitable testing equipment. Here the pin-on-disk apparatus is proven to be the better apparatus to observe friction behavior in nano scale. Nevertheless, the experiments are done in the laboratory and provide a further step in the research of nanoparticles in drilling fluids. The practical application in the field can only be estimated, since many influences like vibration and cutting transportation are eliminated in the laboratory.

Chapter 7
Conclusion

The experimental observations and data analysis of the nanoparticle added drilling fluids allow the following conclustions.

- It exists a coupling effect between temperature and nanoparticles. With increasing temperature the friction reduction can be reduced to a ceratin amount. But this effect is depend on the used nanoparticle material and its physical characteristics in this small scale size.
- Friction factor and wear are directly linked, with increasing friction coefficient increases material wear.
- The interaction between nanoparticles and polymers seems not to significant as assumed. But to be more concrete further tests have to be done.
- Nanoparticles as additive in drilling fluids smoothenes the lubrication process.
- Titania and silica nanoparticles provide efficient lubrication improvements in drilling fluids.
- Lubrication efficiency depends on particle concentration.

Chapter 8
Recommendation for Future Work

The experiments for the pin-on-disk apparatus were promising. Due to the limited number of tests, which are done within this project other investigation aspects can be tested in future experiments:

- higher particle concentration for titania and silica particles in the base fluid.
- longer wear testing time.
- other particle size diameters, since literature says that only a few diameter ranges are beneficial for friction reduction.
- the nanoparticle interaction with polymer fluids to investigate further the interaction between polymers and nanoparticles.
- compact nanoparticles instead of fumed nanoparticles. Both types of particles might differentiate in resistivity towards the applied forces.
- different surface area of the used nanoparticles in comparison with each other to investigate a friction relevant relationship.
- Testing higher temperatures than 50°C for the pin-on-disk apparatus. Since the testing results of the pin-on-disk apparatus are more reliable, other temperature conditions could provide more information about the influence between temperature and lubrication behavior of nanoparticles.

All tests are performed with spherical shaped particles to provide rolling friction in the boundary lubrication stage of the metal to metal contact. One aspect for future research can be the efficiency of nanotube shaped particles in the base fluid.

The usage of nanoparticles in drilling fluids, especially in WBM, is a relativly new idea. Since the material behaviors of the nanoparticles vary strongly from

their microsize behavior all investigations have to be tested without relying on any knowledge the industry has already of the material. Therefore many opportunities and potential for further research exists. All suggested testing ideas could provide a better idea of the field of applications and material properites.

References

[1] Copyright 2013 Petroleum.co.uk . All Rights Reserved. URL http://www.petroleum.co.uk/oil-as-a-lubricant.

[2] URL http://water.me.vccs.edu/concepts/corrosioncauses.html.

[3] Elkem nanosilica 999. Internet, March 2010. URL http://www.elkem.com/Global/ESM/quality-safety/product-data-sheets/polymer-applications/nano-silica999-product-data-sheet.pdf. Product Information Datasheet.

[4] Hydrophilic fumed metal oxides, November 2013. URL https://www.aerosil.com/product/aerosil/en/products/hydrophilic-fumed-metal-oxides/pages/default.aspx.

[5] Hydrophilic fumed silica, November 2013. URL https://www.aerosil.com/lpa-productfinder/page/productsbytext/detail.html?pid=1830&lang=en.

[6] Hydrophilic fumed metal oxides, November 2013. URL https://www.aerosil.com/product/aerosil/en/products/hydrophilic-fumed-metal-oxides/pages/default.aspx.

[7] Abdulaziz Al-Majed SPE Adeleye Sanmi Apaleke, SPE and King Fahd University of Petroleum & Minerals M. Enamul Hossain, SPE. Drilling fluid: State of the art and future trend. *SPE 149555*, page 13, 2012.

[8] Esso Production Research Co. Annis, Max R. High-temperature flow properties of water-based drilling fluids. *Journal of Petroleum Technology*, Volume 19, Number 8(DOI More information: 10.2118/1698-PA):1074–1080, 1967.

[9] *Instruction Manual: MCR Series, Modular Compact Rheometer MCR 52/102/302/502 SmartPave EC-Twist 302 / EC-Starch 302.* Anton Paar, November 2011. Document nr: C92IB001EN-C.

[10] *Instruction Manual: Tribology Measuring Cell T-PTD200.* Anton Paar, March 2012. Document nr: B98ib052EN-L.

[11] E. Richard Booser. *Handbook of Lubrication Theory and Practice of Tribology*, volume Volume 2. CRC Press, 1983. ISBN 0-8493-3902-2 (v.2).

[12] Developed by Subcommittee: G02.40. Standard test method for wear testing with a pin-on-disk apparatus designation: G99-05 (reapproved 2010) din standard: Din50324. International Standardization G99 - 05 (Reapproved 2010), Copyright by ASTM International, 2010.

[13] Andrew W. Batchelor Gwidon W. Stachowiak and Grazyna B. Stachowiak. *Experimental Methods in Tribology*. Copyright Elsevier B.V. All rights reserved, first edition, 2004.

[14] Shell Development Co H.C.H. Darley and Shell Oil Co. R.A. Generes. The use of barium hydroxide in drilling muds. *Published in Petroleum Transaction, AIME*, 207(Document ID : 718-G):252–255, 1956.

[15] K.H. Hiller. Rheological measurements on clay suspensions and drilling fluids at high temperatures and pressures. *Journal of Petroleum Technology*, Volume 15, Number 7(DOI More information: 10.2118/489-PA):779–788, 1963.

[16] Carolin Jahns. Reduced mechanical friction with nanoparticle based drilling fluids. Semester Project at NTNU Trondheim, Norway, June 2013.

[17] Ingrid Solberg Kjellevoll. Casing wear analysis of field experience and current models. Master's thesis, NTNU Trondheim, Department of Petroleum Engineering and Applied Geophysics, June 2013.

[18] Sara Olsson Linn Efsing. Wear testing of high-alloy carbon steel used in mining tools. Master's thesis, KTH Industrial Engineering and Management, Material Science, 2013.

[19] Dr. Wei-Min Liu and Dr. Xiao-Bo Wang. Nanoparticle-based lubricant additives. *Springer-Verlag Berlin Heidelberg 2012*, 10, 2 April 2012.

[20] Jan Mewis and Norman J. Wagner. *Colloidal Suspension Rheology*. Cambridge University Press, 2012.

[21] Esso Production Research Co. Raymond, L.R. Temperature distribution in a circulating drilling fluid. *Journal of Petroleum Technology*, Volume 21, Number 3 (DOI 10.2118/2320-PA):333–341, March 1969.

[22] Halliburton Robello Samuel. Friction factors: What are they for torque, drag, vibration, bottom hole assembly and transient surge/swab analyses? *IADC/SPE 128059*, 11:11, 2010.

[23] George R. Gray Ryen Caenn, H.C.H. Darley. *Composition and Properties of Drilling and Completion Fluids*. Gulf Professional Publishing - an imprint of Elsevier, 6 edition, 2011.

[24] Paal Skalle. Drilling fluid 2013. In *Compendium Lecture Notes: Drilling Fluid*. 2013.

Chapter A

MCR - Tribology Measurement Data

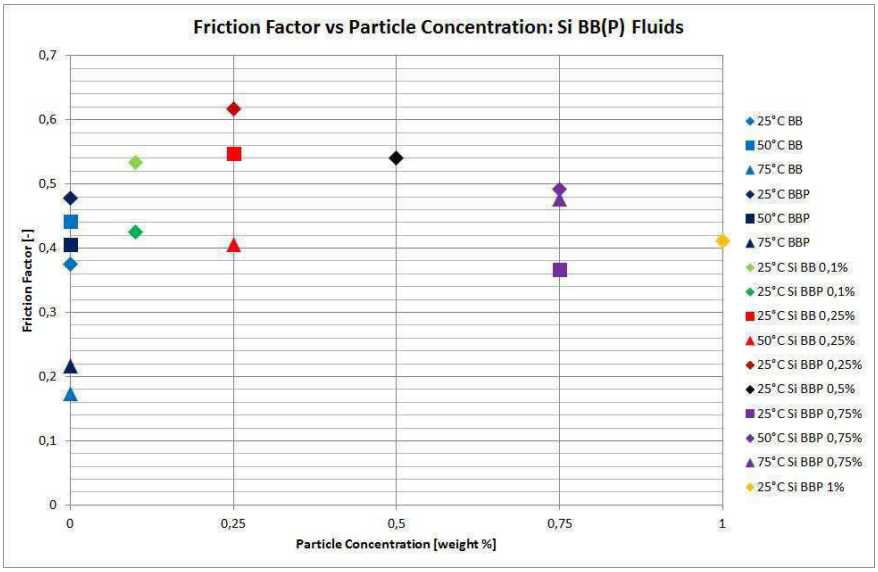

Figure A.1: Friction Factor depending on the added particle concentration of silica

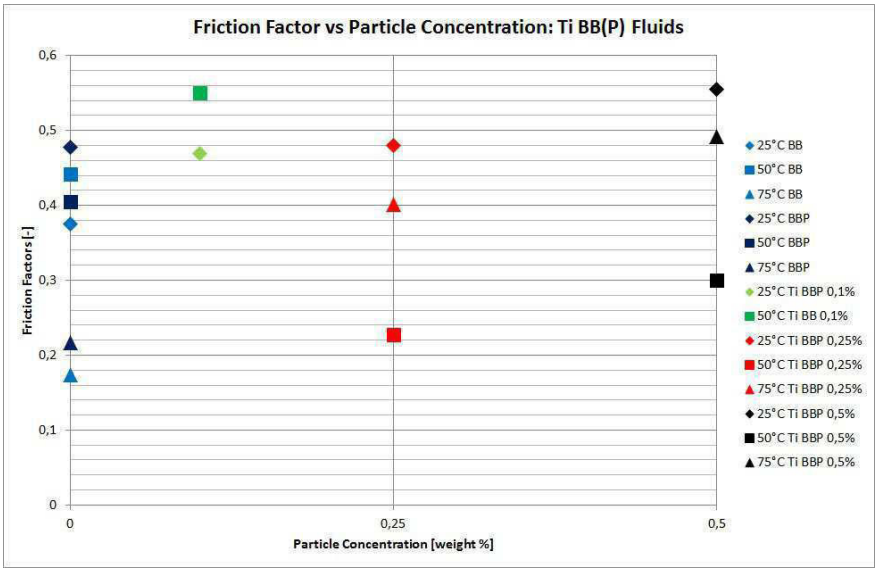

Figure A.2: Friction Factor depending on the added particle concentration of titania

Table A.1: Average friction coefficient values for each speed range of BB

RPM	**25°C**	**50°C**	**75°C**
3	0,376	0,442	0,174
6	0,471	0,458	0,453
100	0,359	0,351	0,362
200	0,341	0,347	0,396
300	0,332	0,343	0,387
600	0,344	0,380	0,371
Average	0,371	0,387	0,357

Table A.2: Average friction coefficient values for each speed range of BBP

RPM	**25°C**	**50°C**	**75°C**
3	0,478	0,405	0,217
6	0,437	0,493	0,482
100	0,305	0,373	0,370
200	0,301	0,351	0,397
300	0,316	0,355	0,371
600	0,329	0,356	0,384
Average	0,361	0,389	0,370

Table A.3: Average friction coefficient values for each speed range of 0,1 weight% silica BBP Fluid

RPM	**25°C**
3	0,426
6	0,573
100	0,387
200	0,355
300	0,352
600	0,374
Average	0,411

Table A.4: Average friction coefficient values for each speed range of 0,1 weight% silica BB Fluid

RPM	**25°C**
3	0,534
6	0,620
100	0,374
200	0,354
300	0,355
600	0,378
Average	0,436

Table A.5: Average friction coefficient values for each speed range of 0,25 weight% Silica BBP Fluid

RPM	**25°C**
3	0,617
6	0,529
100	0,404
200	0,368
300	0,364
600	0,367
Average	0,441

Table A.6: Average friction coefficient values for each speed range of 0,25 weight% silica BB Fluid

RPM	**25°C**	**50°C**
3	0,548	0,406
6	0,529	0,569
100	0,348	0,414
200	0,353	0,396
300	0,365	0,404
600	0,369	0,449
Average	0,419	0,440

Table A.7: Average friction coefficient values for each speed range of 0,5 weight% silica BBP Fluid

RPM	**25°C**
3	0,540
6	0,496
100	0,377
200	0,375
300	0,383
600	0,373
Average	0,424

Table A.8: Average friction coefficient values for each speed range of 0,75 weight% silica BBP Fluid

RPM	**25°C**	**50°C**	**75°C**
3	0,367	0,491	0,477
6	0,479	0,614	0,573
100	0,390	0,407	0,437
200	0,369	0,398	0,418
300	0,363	0,395	0,435
600	0,368	0,409	0,478
Average	0,390	0,452	0,470

Table A.9: Average friction coefficient values for each speed range of 1 weight% silica BBP Fluid

RPM	**25°C**
3	0,411
6	0,516
100	0,413
200	0,387
300	0,388
600	0,401
Average	0,419

Table A.10: Average friction coefficient values for each speed range of 0,1 weight% alumina BBP Fluid

RPM	**25°C**	**50°C**	**75°C**
3	0,448	0,319	0,472
6	0,532	0,556	0,587
100	0,404	0,417	0,426
200	0,360	0,405	0,441
300	0,352	0,409	0,428
600	0,387	0,421	0,473
Average	0,414	0,421	0,471

Table A.11: Average friction coefficient values for each speed range of 0,1 weight% alumina BB Fluid

RPM	**25°C**
3	0,458
6	0,608
100	0,396
200	0,360
300	0,347
600	0,391
Average	0,427

Table A.12: Average friction coefficient values for each speed range of 0,25 weight% alumina BBP Fluid

RPM	**25°C**	**50°C**	**75°C**
3	0,508	0,479	0,224
6	0,539	0,540	0,507
100	0,386	0,390	0,438
200	0,355	0,387	0,452
300	0,359	0,390	0,450
600	0,380	0,424	0,466
Average	0,421	0,435	0,423

Table A.13: Average friction coefficient values for each speed range of 0,25 weight% alumina BB Fluid

RPM	**25°C**	**50°C**	**75°C**
3	0,546	0,508	0,204
6	0,581	0,574	0,468
100	0,390	0,402	0,477
200	0,362	0,388	0,409
300	0,372	0,400	0,369
600	0,400	0,430	0,465
Average	0,442	0,450	0,399

Table A.14: Average friction coefficient values for each speed range of 0,5 weight% alumina BBP Fluid

RPM	**25°C**	**50°C**	**75°C**
3	0,546	0,524	0,112
6	0,583	0,604	0,296
100	0,367	0,391	0,431
200	0,382	0,388	0,443
300	0,358	0,388	0,405
600	0,389	0,417	0,454
Average	0,438	0,452	0,357

Table A.15: Average friction coefficient values for each speed range of 0,75 weight% alumina BBP Fluid

RPM	**25°C**	**50°C**	**75°C**
3	0,581	0,511	0,148
6	0,528	0,596	0,376
100	0,368	0,415	0,425
200	0,347	0,384	0,450
300	0,352	0,404	0,394
600	0,400	0,427	0,445
Average	0,429	0,456	0,373

Table A.16: Average friction coefficient values for each speed range of 0,1 weight% titania BBP Fluid

RPM	**25°C**
3	0,469
6	0,518
100	0,389
200	0,349
300	0,355
600	0,385
Average	0,411

Table A.17: Average friction coefficient values for each speed range of 0,1 weight% titania BB Fluid

RPM	**25°C**
3	0,550
6	0,565
100	0,386
200	0,370
300	0,387
600	0,389
Average	0,441

Table A.18: Average friction coefficient values for each speed range of 0,25 weight% titania BBP Fluid

RPM	**25°C**	**50°C**	**75°C**
3	0,480	0,227	0,402
6	0,560	0,597	0,596
100	0,400	0,411	0,442
200	0,358	0,381	0,413
300	0,361	0,400	0,409
600	0,385	0,415	0,411
Average	0,424	0,405	0,445

Table A.19: Average friction coefficient values for each speed range of 0,5 weight% titania BBP Fluid

RPM	**25°C**	**50°C**	**75°C**
3	0,555	0,300	0,492
6	0,643	0,486	0,591
100	0,454	0,406	0,410
200	0,434	0,395	0,429
300	0,431	0,398	0,408
600	0,446	0,438	0,483
Average	0,494	0,404	0,469

Chapter B
Pin-on-Disk Measurement Data

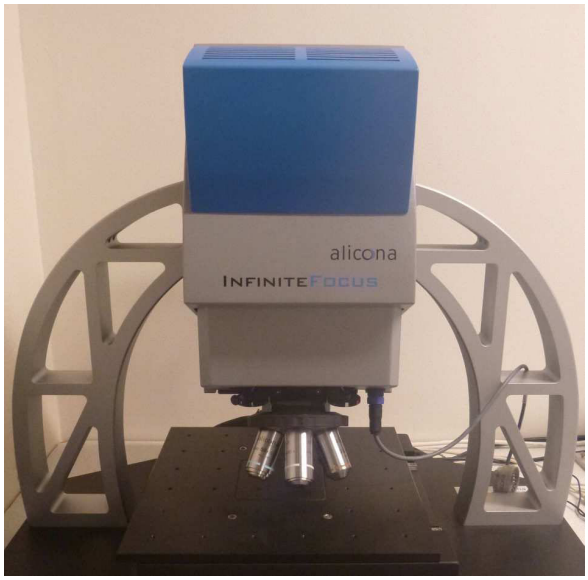

Figure B.1: Optical 3D confocal microscope; Company: alicona Type: InfiniteFocus

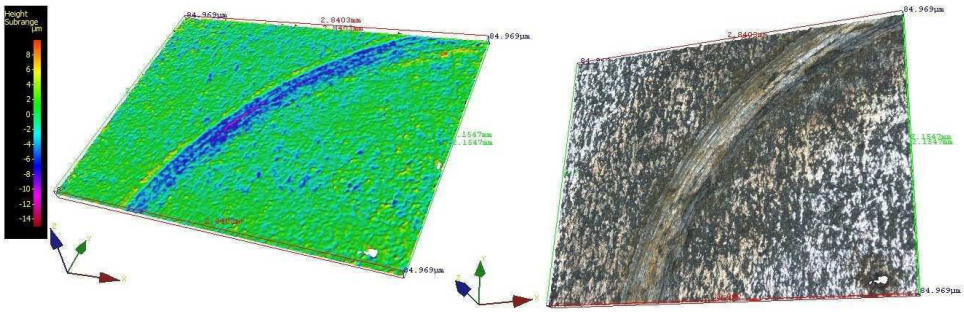

Figure B.2: Image of the BB fluid with 0,5weight% added silica particles, Test 1 50°C

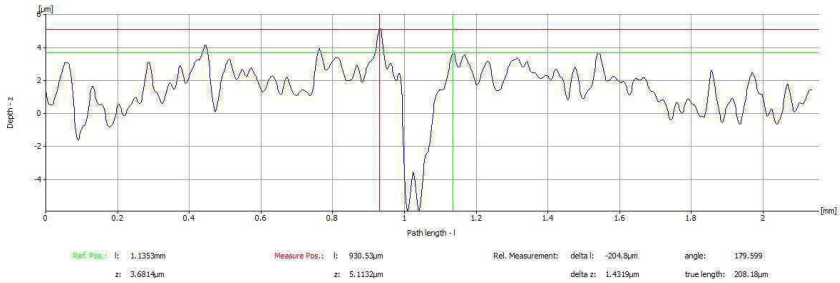

Figure B.3: Profile of the BB fluid with 0,5weight% added silica particles, Test 1 50°C

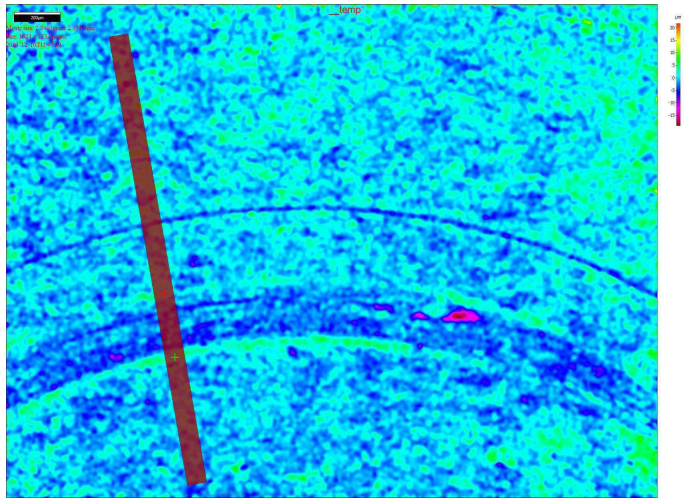

Figure B.4: Image of the BB fluid with 0,25 weight% added titania particles, Test 1 50°C

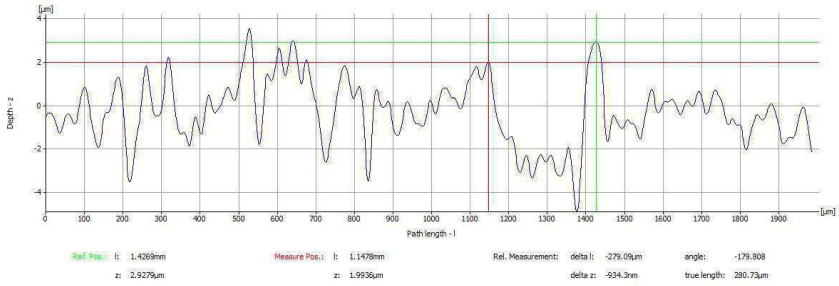

Figure B.5: Profile of the BB fluid with 0,25weight% added titania particles, Test 1 50°C

Chapter C

MCR - Viscometer Measurement Data

Table C.1: 25°C BB fluid

Meas. Pts.	Time [s]	Shear Stress [Pa]	Viscosity [Pas]	Speed [1/min]	Torque [μNm]
1	16,6	22,2	5,73	3	1110
1	32,9	21,6	2,79	6	1080
1	53,9	25,5	0,198	100	1280
1	73,5	28,3	0,11	200	1420
1	90,8	29,9	0,0772	300	1500
1	104	35,8	0,0462	600	1790

Table C.2: 50°C BB fluid

Meas. Pts.	Time [s]	Shear Stress [Pa]	Viscosity [Pas]	Speed [1/min]	Torque [μNm]
1	27,8	22,6	4,44	3,95	1130
1	45,1	22,7	2,22	7,91	1130
1	79,4	26,4	0,155	132	1320
1	106	28,8	0,0846	264	1440
1	127	30,2	0,0591	395	1510
1	147	35	0,0343	791	1750

Table C.3: 75°C BB fluid

Meas. Pts.	Time [s]	Shear Stress [Pa]	Viscosity [Pas]	Speed [1/min]	Torque [μNm]
1	16,6	36,8	7,21	3,95	1840
1	30,5	37,1	3,64	7,91	1860
1	48,1	39,5	0,232	132	1980
1	69	41,6	0,122	264	2080
1	83,9	43,5	0,0853	395	2180
1	105	45	0,0441	791	2250

Table C.4: 25°C BBP fluid

Meas. Pts.	Time [s]	Shear Stress [Pa]	Viscosity [Pas]	Speed [1/min]	Torque [μNm]
1	37,7	12,5	2,45	3,95	625
1	54,2	12,8	1,26	7,91	644
1	71,6	16,7	0,0983	132	837
1	85,5	20,1	0,0591	264	1010
1	98,1	22,6	0,0444	395	1130
1	114	29,4	0,0288	791	1470

Table C.5: 50°C BBP

Meas. Pts.	Time [s]	Shear Stress [Pa]	Viscosity [Pas]	Speed [1/min]	Torque [μNm]
1	15,8	16	3,15	3,95	803
1	29,1	16,5	1,62	7,91	827
1	53,4	20,3	0,12	132	1020
1	79,2	22,2	0,0652	264	1110
1	100	23,9	0,0468	395	1190
1	120	29,1	0,0285	791	1460

Table C.6: 75°C BBP

Meas. Pts.	Time [s]	Shear Stress [Pa]	Viscosity [Pas]	Speed [1/min]	Torque [μ Nm]
1	57,7	35,4	6,94	3,95	1770
1	74,2	34,6	3,4	7,91	1740
1	101	33,3	0,196	132	1670
1	122	35,3	0,104	264	1770
1	137	37,2	0,0729	395	1860
1	158	38,3	0,0376	791	1920

Table C.7: 25°C alumina added BB fluid, 0,5 weight%

Meas. Pts.	Time [s]	Shear Stress [Pa]	Viscosity [Pas]	Speed [1/min]	Torque [μNm]
1	13,3	65,9	17	3	3300
1	28,6	64,2	8,3	6	3210
1	41,5	57,5	0,446	100	2880
1	53,1	62,1	0,241	200	3110
1	64,7	66	0,17	300	3300
1	81,7	74,5	0,0962	600	3730

Table C.8: 50°C alumina added BB fluid, 0,5 weight%

Meas. Pts.	Time [s]	Shear Stress [Pa]	Viscosity [Pas]	Speed [1/min]	Torque [μNm]
1	27,8	70,1	18,1	3	3510
1	43,4	85,5	11,1	6	4280
1	60,5	86,4	0,67	100	4330
1	74,9	85,1	0,33	200	4260
1	86,5	84,8	0,219	300	4250
1	98,1	85,9	0,111	600	4300

Table C.9: 25°C alumina added BBP fluid, 0,75 weight%

Meas. Pts.	Time [s]	Shear Stress [Pa]	Viscosity [Pas]	Speed [1/min]	Torque [μNm]
1	16,3	48,2	9,46	3,95	2420
1	28,4	46,5	4,56	7,91	2330
1	44,4	44	0,259	132	2200
1	58,3	47,5	0,14	264	2380
1	69,9	50,2	0,0985	395	2520
1	102	54	0,0529	791	2700

Table C.10: 50°C alumina added BBP fluid, 0,75 weight%

Meas. Pts.	Time [s]	Shear Stress [Pa]	Viscosity [Pas]	Speed [1/min]	Torque [μNm]
1	11,6	63	12,3	3,95	3150
1	27	73,4	7,2	7,91	3680
1	40,9	69,1	0,407	132	3460
1	52,5	69,1	0,203	264	3460
1	64,1	68,9	0,135	395	3450
1	75,7	71,3	0,0699	791	3570

Table C.11: 75°C alumina added BBP fluid, 0,75 weight%

Meas. Pts.	Time [s]	Shear Stress [Pa]	Viscosity [Pas]	Speed [1/min]	Torque [μNm]
1	24,1	87,9	17,2	3,95	4400
1	39,7	96,8	9,49	7,91	4850
1	53,7	95,4	0,561	132	4780
1	68,2	92,7	0,273	264	4640
1	83,8	91,3	0,179	395	4570
1	95,4	92,7	0,0909	791	4640

Table C.12: 25°C silica added BBP fluid, 0,1 weight%

Meas. Pts.	Time [s]	Shear Stress [Pa]	Viscosity [Pas]	Speed [1/min]	Torque [μNm]
1	14,9	21	4,13	3,95	1050
1	29,6	21,9	2,15	7,91	1100
1	47	28,2	0,166	132	1410
1	59,4	32,9	0,0967	264	1650
1	73,2	36,3	0,0712	395	1820
1	91,5	44,1	0,0432	791	2210

Table C.13: 50°C silica added BBP fluid, 0,1 weight%

Meas. Pts.	Time [s]	Shear Stress [Pa]	Viscosity [Pas]	Speed [1/min]	Torque [μNm]
1	17,8	25,8	5,06	3,95	1290
1	32	26	2,55	7,91	1300
1	62,8	31,1	0,183	132	1560
1	79,3	34,4	0,101	264	1720
1	94,1	37,3	0,0731	395	1870
1	110	43,6	0,0428	791	2180

Table C.14: 75°C silica added BBP fluid, 0,1 weight%

Meas. Pts.	Time [s]	Shear Stress [Pa]	Viscosity [Pas]	Speed [1/min]	Torque [μNm]
1	27,9	37,8	7,41	3,95	1890
1	44,5	37,5	3,68	7,91	1880
1	64,9	42,3	0,249	132	2120
1	89,7	44,3	0,13	264	2220
1	112	44,6	0,0875	395	2240
1	127	49,1	0,0481	791	2460

Table C.15: 25°C silica added BBP fluid, 1 weight%

Meas. Pts.	Time [s]	Shear Stress [Pa]	Viscosity [Pas]	Speed [1/min]	Torque [μNm]
1	14,8	19,7	3,87	3,95	989
1	30	20,8	2,04	7,91	1040
1	44,6	27,7	0,163	132	1390
1	57,1	33	0,0969	264	1650
1	71,4	36,8	0,0722	395	1840
1	90,1	45,7	0,0449	791	2290

Table C.16: 50°C silica added BBP fluid, 1 weight%

Meas. Pts.	Time [s]	Shear Stress [Pa]	Viscosity [Pas]	Speed [1/min]	Torque [μNm]
1	21,6	23,9	4,69	3,95	1200
1	35,4	24	2,36	7,91	1200
1	56,9	29,4	0,173	132	1470
1	71,1	32,5	0,0955	264	1630
1	85,9	35,6	0,0697	395	1780
1	101	42,6	0,0417	791	2130

Table C.17: 75°C silica added BBP fluid, 1 weight%

Meas. Pts.	Time [s]	Shear Stress [Pa]	Viscosity [Pas]	Speed [1/min]	Torque [μNm]
1	14,9	35,5	6,97	3,95	1780
1	31,6	43	4,21	7,91	2150
1	48,5	41,8	0,246	132	2090
1	61,2	44,8	0,132	264	2240
1	76,1	46,4	0,091	395	2320
1	96,5	50,6	0,0496	791	2540

Table C.18: 25°C titania added BB fluid, 0,1 weight%

Meas. Pts.	Time [s]	Shear Stress [Pa]	Viscosity [Pas]	Speed [1/min]	Torque [μNm]
1	15,7	24,4	6,31	3	1220
1	28,3	25,3	3,27	6	1270
1	46,1	29,7	0,23	100	1490
1	67,8	31,8	0,123	200	1590
1	84,8	31,9	0,0825	300	1600
1	99,9	37,6	0,0485	600	1880

Table C.19: 25°C titania added BB fluid, 0,5 weight%

Meas. Pts.	Time [s]	Shear Stress [Pa]	Viscosity [Pas]	Speed [1/min]	Torque [μNm]
1	12,3	26,9	6,96	3	1350
1	24,7	26,6	3,44	6	1330
1	44,2	30,3	0,235	100	1520
1	60,6	33,1	0,128	200	1660
1	82,6	34	0,088	300	1710
1	96,9	39,1	0,0505	600	1960